Spin-valley collective modes of the electron liquid in graphene

Zachary M. Raines [1], Vladimir I. Fal'ko,[2,3,4] and Leonid I. Glazman [1]
[1]*Department of Physics, Yale University, New Haven, Connecticut 06520, USA*
[2]*National Graphene Institute, University of Manchester, Manchester M13 9PL, United Kingdom*
[3]*Department of Physics, University of Manchester, Manchester M13 9PL, United Kingdom*
[4]*Henry Royce Institute for Advanced Materials, Manchester M13 9PL, United Kingdom*

(Received 10 November 2020; revised 29 January 2021; accepted 2 February 2021; published 15 February 2021)

We develop the theory of collective modes supported by a Fermi liquid of electrons in pristine graphene. Under reasonable assumptions regarding the electron-electron interaction, all the modes but the plasmon are overdamped. In addition to the $SU(2)$-symmetric spin mode, these include also the valley imbalance modes obeying a $U(1)$ symmetry, and a $U(2)$-symmetric valley spin imbalance mode. We derive the interactions and diffusion constants characterizing the overdamped modes. The corresponding relaxation rates set fundamental constraints on graphene valley- and spintronics applications.

DOI: 10.1103/PhysRevB.103.075422

I. INTRODUCTION

An extremely long electron mean free path [1] combined with a fairly strong electron-electron interaction [2] makes graphene an interesting platform for investigating Fermi liquid effects in solids. The strength of interaction may be tuned by varying the electron density with respect to the neutrality point in graphene and by changing the dielectric environment encapsulating the graphene sheet. A hallmark of Fermi liquid behavior is an emergence of the collective modes associated with the symmetries of the system. The charge density mode, the plasmon, is the easiest to couple to, and can be probed in various spectroscopic experiments [3]. Plasmons are protected from Landau damping by their high propagation velocity, leading to fairly narrow spectroscopic lines. The spectra of plasmons have been calculated for and measured in various settings [3–5].

More recently, hydrodynamic electron flow has attracted much attention, occurring in the regime where the electron-electron mean free path is much smaller than other collision scales, $\ell_{e\text{-}e} \ll \ell$. In the absence of disorder, a uniform electric current is protected by charge conservation and translation invariance, but a nonuniform electron flow is associated with size effects which arise from the electron viscosity. To find it, one needs to solve the two-dimensional Fermi liquid kinetic equation [6,7] for the quasiparticle distribution function. A variety of hydrodynamic size effects have been predicted and addressed experimentally in electric DC transport [7–11].

A fairly weak spin-orbit interaction in carbon leaves electron spin in graphene approximately conserved. Furthermore, the two Dirac points in graphene's electron spectrum are located far from each other in the Brillouin zone. As the result, electron scattering between the valleys associated with the Dirac points is suppressed. The approximate conservation of the spin and valley indices of a quasiparticle raises the question of the existence of sound modes in these channels. It has also given rise to a host of proposals for "spintronics" and "valleytronics" graphene applications [12,13] exploiting in various ways spin or valley currents. The valleytronics proposals are specific for multivalley materials, while the spintronics ones are a part of a broader semiconductor physics literature [14,15]. In the analysis of spin- and valley-current conservation, the majority of theory works consider the effect of static disorder scattering noninteracting electrons at the Fermi level (see, e.g., Refs. [15,16]). A notable exception is Ref. [17], which evaluated in the Born approximation the spin relaxation rate due to electron-electron collisions in a two-dimensional electron gas, partially spin polarized by a magnetic field. Later this theory was applied to analyze the measurement of spin diffusion in the absence of polarizing magnetic field [18]. We note in passing that the spin diffusion in the $SU(2)$-symmetric neutral three-dimensional Fermi liquid was considered in the context of the low-temperature He-3 properties [19,20], and for ungapped graphene in two dimensions [21].

In this work, we study dynamics of the neutral modes supported by the electron Fermi liquid in graphene. The neutral modes include an $SU(2)$-symmetric spin mode, $U(1)$-symmetric modes of the intervalley coherence and imbalance, as well as $U(2)$-symmetric intervalley spin modes. We identify and estimate the relative strength of the microscopic interactions which determine the values of parameters in a phenomenological Fermi liquid theory for these modes. Under reasonable assumptions, all of the neutral modes are overdamped, and there is no neutral zero or first sound. The spread and decay of the spin-polarization density and of the intervalley coherence and imbalance densities are thus characterized by their diffusion constants. To find the diffusion constants, we evaluate the corresponding transport relaxation rates from the linearized collision integral which accounts for the electron-electron scattering and solve the linearized kinetic equations. The obtained rates depend on the temperature, electron density, and gaps at the Dirac points. These gaps may

appear due to deformation of the graphene lattice, for example, in graphene encapsulated in hexagonal boron nitride [22], and have a profound effect on electron backscattering due to the Berry flux redistribution across the Brillouin zone. Indeed, backscattering of electrons in graphene may only occur in the presence of such gaps [23,24].

II. MODEL

A realistic level of the electron density induced by electrostatic gating corresponds to fairly small Fermi wave vectors $k_F \ll |\mathbf{K}|$ (measured from the respective Dirac points). Therefore, we adopt the description of the electron system in terms of slowly-varying-in-space Fermi fields [25,26]:

$$\hat{\Psi}_\sigma(\mathbf{r}) = u_{KA}(\mathbf{r})\, u_{KB}(\mathbf{r})\, u_{K'B}(\mathbf{r}) \; - u_{K'A}(\mathbf{r}) \cdot \hat{\vec{\psi}}_\sigma(\mathbf{r}), \qquad (1)$$

where $u_{\mathbf{k}\Sigma}(\mathbf{r})$ are the Bloch wavefunctions concentrated near the $\Sigma = A, B$ sublattice sites, at the $\mathbf{k} = \mathbf{K}, \mathbf{K}'$ points in the Brillouin zone. For definiteness, we consider the Fermi level above the Dirac point. We may then perform a projection onto the conduction band $\vec{\psi}_{\mathbf{k}\sigma} = \sum_\zeta \chi_{\mathbf{k}\zeta} c_{\mathbf{k}\zeta\sigma}$ where the sublattice pseudospinors $\chi_{\mathbf{k},\zeta}$ are eigenvectors of the Dirac Hamiltonian,

$$(v\mathbf{k}\cdot\boldsymbol{\Sigma} + \zeta\Delta\Sigma_3)\chi_{\mathbf{k}\zeta} = \sqrt{v^2k^2+\Delta^2}\,\chi_{\mathbf{k}\zeta}, \qquad (2)$$

with v the Dirac velocity and Σ_i the Pauli matrices in sublattice space [27]. In terms of the upper-band operators, the low-energy Hamiltonian is

$$\hat{H} = \sum_{\mathbf{k}\zeta\sigma}[\sqrt{v^2k^2+\Delta^2} - (\Delta + E_F)]c^\dagger_{\mathbf{k}\zeta\sigma}c_{\mathbf{k}\zeta\sigma} + \hat{H}_{\rm int}, \qquad (3)$$

where ζ and σ are respectively the valley and spin indices, E_F is the Fermi level measured from the gap edge, and the interaction Hamiltonian is

$$\hat{H}_{\rm int} = \frac{1}{2}\sum_{\mathbf{k},\mathbf{k}',\mathbf{q}}\sum_{\substack{\zeta_1\zeta_1'\zeta_2\zeta_2'\\ \sigma_1\sigma_1'\sigma_2\sigma_2'}} U^{\zeta_1\zeta_1';\zeta_2;\zeta_2'}_{\sigma_1\sigma_1';\sigma_2;\sigma_2}(\mathbf{k},\mathbf{k}',\mathbf{q}) \times :c^\dagger_{\zeta_1\sigma_1}(\mathbf{k}+\mathbf{q})c_{\zeta_1'\sigma_1'}(\mathbf{k})c^\dagger_{\zeta_2\sigma_2}(\mathbf{k}'-\mathbf{q})c_{\zeta_2'\sigma_2'}(\mathbf{k}'):, \qquad (4)$$

where $:\cdots:$ denotes normal ordering with respect to the electron operators c. The valley charge and spin symmetries constrain the short-range interactions to be of the form (see Appendix A)

$$\begin{aligned} U(\mathbf{p},\mathbf{p}',\mathbf{q}) = {} & U^d_{\mathbf{p},\mathbf{p}',\mathbf{q}} + U^s_{\mathbf{p},\mathbf{p}',\mathbf{q}}\boldsymbol{\sigma}\cdot\boldsymbol{\sigma} \\ & + U^{v\parallel}_{\mathbf{p},\mathbf{p}',\mathbf{q}}\boldsymbol{\tau}^\parallel\cdot\boldsymbol{\tau}^\parallel + U^{vz}_{\mathbf{p},\mathbf{p}',\mathbf{q}}\tau^3\tau^3 \\ & + U^{m\parallel}_{\mathbf{p},\mathbf{p}',\mathbf{q}}\boldsymbol{\tau}^\parallel\cdot\boldsymbol{\tau}^\parallel\boldsymbol{\sigma}\cdot\boldsymbol{\sigma} + U^{mz}_{\mathbf{p},\mathbf{p}',\mathbf{q}}\tau^3\tau^3\boldsymbol{\sigma}\cdot\boldsymbol{\sigma}, \end{aligned} \qquad (5)$$

where τ^i and σ^i are Pauli matrices in valley and spin space, respectively, and all of the functions U^α are short ranged except for U^d which includes the long-range part of the Coulomb interaction, $V(q)$. The six functions, $U^\alpha_{\mathbf{p},\mathbf{p}',\mathbf{q}}$, are the inputs of our theory. These, in turn, can be expressed in terms of the interaction constants g_{zz}, $g_{\perp\perp}$, $\widetilde{g}_{00}$ of an unprojected Hamiltonian [26] and screened Coulomb potential $V(q)$, combined with the matrix elements of the projection operator constructed from eigenspinors $\chi_{\mathbf{k}\zeta}$. The latter contribute to the dependence of $U(\mathbf{p},\mathbf{p}',\mathbf{q})$ on the respective momenta (cf. Appendix A).

The space-group symmetry of the graphene lattice constrains the form of the interaction Hamiltonian. Allowing for the presence of a long-range density-density interaction, and neglecting the overlap of the Bloch functions on the A and B sublattices, the interaction Hamiltonian in terms of the unprojected operators $\psi_{k\zeta}$ in Eq. (1) takes the form [27] (cf. Ref. [26])

$$\begin{aligned} \hat{H}^\psi_{\rm int} = {} & \frac{1}{2}\sum_{\mathbf{r},\mathbf{r}'} V(\mathbf{r}-\mathbf{r}') :\psi^\dagger(\mathbf{r})\psi(\mathbf{r})\psi^\dagger(\mathbf{r}')\psi(\mathbf{r}'): \\ & + \frac{1}{2}\sum_{\mathbf{r}}\sum_{\alpha\beta}[g_{\alpha\beta}:\psi^\dagger(\mathbf{r})\Sigma^\alpha\tau^\beta\psi(\mathbf{r})\psi^\dagger(\mathbf{r}')\Sigma^\alpha\tau^\beta\psi(\mathbf{r}'): \\ & + \tilde{g}_{00}:\psi^\dagger(\mathbf{r})\Sigma^z\tau^z\psi(\mathbf{r})\psi^\dagger(\mathbf{r}')\psi(\mathbf{r}'):], \end{aligned} \qquad (6)$$

with only $\tilde{g}_{00}$, g_{zz}, and $g_{\perp\perp} = g_{xx} = g_{xy} = g_{yx} = g_{yy}$ nonzero in the second term. Projecting onto the upper bands reproduces the $U(2)\times U(2)$ symmetric form of the interaction, Eq. (5). The interaction functions in Eq. (5) can then be expressed in terms of the interaction constants g_{zz}, $g_{\perp\perp}$, $\widetilde{g}_{00}$, and the function $V(q)$ combined with matrix elements of the eigenspinors $\chi_{\mathbf{k}\zeta}$ (see Appendix A).

One may estimate the interaction parameters here in terms of the matrix elements of the screened Coulomb interaction $V(q)$. To the lowest order one finds

$$g_{\perp\perp} \sim V(|\mathbf{K}-\mathbf{K}'|),\;\; g_{zz} \sim V(|\mathbf{b}|),\;\; \tilde{g}_{00} \sim \frac{g_{zz}\Delta}{v_F|\mathbf{K}-\mathbf{K}'|}. \qquad (7)$$

Like the Dirac gap Δ, the constant $\tilde{g}_{00}$ is nonzero only if the lattice C_6 symmetry is broken. From the hierarchy of scales $q_{\rm TF}, k_F \ll |\mathbf{K}-\mathbf{K}'|$, we then have

$$V(q\sim k_F) \gg g_{\perp\perp} > g_{zz} > \tilde{g}_{00} \qquad (8)$$

(here $q_{\rm TF}$ and k_F are respectively the Thomas-Fermi and Fermi wave vectors).

III. LANDAU-FERMI LIQUID THEORY OF GRAPHENE AWAY FROM THE CHARGE NEUTRALITY POINT

The form of the interaction Hamiltonian, Eq. (5), stipulates an identical matrix form of the Landau functions $f(\mathbf{p}\cdot\mathbf{p}')$ of the phenomenological Fermi liquid theory. It also motivates the introduction of collective coordinates

$$\begin{aligned} n(\mathbf{r},\mathbf{p}) &= \frac{1}{G_sG_v}{\rm tr}\hat{\rho}(\mathbf{r},\mathbf{p}), \\ \mathbf{s}(\mathbf{r},\mathbf{p}) &= \frac{1}{G_sG_v}{\rm tr}\hat{\boldsymbol{\sigma}}\hat{\rho}(\mathbf{r},\mathbf{p}), \\ \mathbf{Y}(\mathbf{r},\mathbf{p}) &= \frac{1}{G_sG_v}{\rm tr}\hat{\boldsymbol{\tau}}\hat{\rho}(\mathbf{r},\mathbf{p}), \\ M^j_i(\mathbf{r},\mathbf{p}) &= \frac{1}{G_sG_v}{\rm tr}\hat{\tau}_i\hat{\sigma}_j\hat{\rho}(\mathbf{r},\mathbf{p}), \end{aligned} \qquad (9)$$

in terms of the Wigner transformed single particle density matrix $\hat{\rho}(\mathbf{r},\mathbf{q})$, which may be interpreted as charge n, spin $\mathbf{s}$, valley pseudospin $\mathbf{Y}$, and spin-triplet valley pseudospin $\mathbf{M}_i$; G_s and G_v are spin and valley degeneracy, respectively. In particular, as we will see below, the linear kinetic equation decouples in terms of these coordinates, such that each collective mode obeys an equation depending only on that channel.

For compactness, it is useful to define the arrays $\hat{X}^\mu$, ρ^μ, and f^μ with multi-index $\mu = (\alpha, \beta)$:

$$\hat{X}^{\alpha\beta} = \hat{\tau}^\alpha \hat{\sigma}^\beta, \quad \rho^{00} = n, \quad \rho^{0i} = s_i, \quad \rho^{i0} = Y_i, \quad \rho^{ij} = M_i^j,$$
$$f^{00} = f_d, \quad f^{0i} = f_s, \quad f^{i=1,2;0} = f_{v\parallel},$$
$$f^{3;0} = f_{vz}, \quad f^{i=1,2;j} = f_{m\parallel}, \quad f^{3;i} = f_{mz}.$$

Here we have introduced the Landau functions $f_i(\mathbf{p}\cdot\mathbf{p}')$ for each channel. This allows us to write the Landau quasiparticle energy matrix as

$$\hat{\epsilon}(\mathbf{p},\mathbf{r}) = \xi(\mathbf{p})\hat{X}^{00} + \varphi^\mu(\mathbf{r})\hat{X}^\mu + \sum_{\mathbf{p}'}\sum_\mu \hat{X}^\mu f^\mu(\mathbf{p}\cdot\mathbf{p}')\hat{\rho}^\mu(\mathbf{r},\mathbf{p}'), \tag{10}$$

where $\xi(\mathbf{k})$ is the free particle excitation energy and $\varphi^\mu(\mathbf{r})$ is a generalized potential conjugate to ρ^μ (for the density channel this includes the self-consistent Vlasov field).

We may obtain linearized equations of motion for each of the collective coordinates from the Landau-Silin kinetic equation

$$\frac{\partial\hat{\rho}}{\partial t} + \frac{1}{2}\left\{\frac{\partial\hat{\epsilon}}{\partial\mathbf{p}}, \frac{\partial\hat{\rho}}{\partial\mathbf{r}}\right\} - \frac{1}{2}\left\{\frac{\partial\hat{\epsilon}}{\partial\mathbf{r}}, \frac{\partial\hat{\rho}}{\partial\mathbf{p}}\right\} + i[\hat{\epsilon},\hat{\rho}] = \hat{I}[\hat{\rho}], \tag{11}$$

where $I[\hat{\rho}]$ is the collision integral. We introduce the linearized deviation $\hat{\rho}(\mathbf{k},\mathbf{r}) = n_F(\bar{\epsilon}(\mathbf{k})) + \delta\hat{\rho}(\mathbf{k},\mathbf{r})$, where we have defined the self-consistently determined local equilibrium energy $\bar{\epsilon}(\mathbf{k}) = \epsilon[n_F(\bar{\epsilon}(\mathbf{k}))]$ via Eq. (10). Expanding Eq. (11) to linear order in $\delta\rho$, one may take traces of the equation multiplied by the matrices $\hat{X}^\mu$, as in Eq. (9), to obtain

$$\frac{\partial\delta\rho^\mu(\mathbf{k},\mathbf{r})}{\partial t} + \mathbf{v}\cdot\frac{\partial}{\partial\mathbf{r}}\delta\bar{\rho}^\mu(\mathbf{k},\mathbf{r}) + \left.\frac{\partial n}{\partial\epsilon}\right|_{\bar{\epsilon}}\mathbf{v}\cdot\boldsymbol{\mathcal{F}}^\mu = \frac{1}{G_sG_v}\mathrm{tr}\hat{X}^\mu\hat{I}[\delta\hat{\rho}], \tag{12}$$

with generalized forces $\boldsymbol{\mathcal{F}}^\mu = -\nabla\varphi^\mu$, linearized deviations in each channel,

$$\delta\rho^\mu(\mathbf{r},\mathbf{p}) = \rho^\mu(\mathbf{r},\mathbf{p}) - n_F(\bar{\epsilon}(\mathbf{k}))\delta_{\mu,00}, \tag{13}$$

and deviation from local equilibrium [28],

$$\delta\bar{\rho}^\mu(\mathbf{k},\mathbf{r}) = \delta\rho^\mu(\mathbf{k},\mathbf{r}) - \left.\frac{\partial n}{\partial\epsilon}\right|_{\bar{\epsilon}} G_sG_v\sum_{\mathbf{p}} f^\mu(\mathbf{k}\cdot\mathbf{p})\delta\rho^\mu(\mathbf{p},\mathbf{r}). \tag{14}$$

Note that while the Berry connection contributes to the full kinetic equation [29], it does not enter the linearized equations of motion as long as we are interested in long-wavelength responses [30].

At low temperatures $T \ll T_F$ the derivative of the Fermi function is sharply peaked at the Fermi level, pinning energies to the Fermi surface. We therefore reparametrize the linearized deviations and Fermi liquid functions

$$\delta\rho^\mu(\mathbf{p},\mathbf{r}) \equiv -\left.\frac{\partial n}{\partial\epsilon}\right|_{\bar{\epsilon}}\nu^\mu(\phi,\mathbf{r}) \tag{15}$$

in terms of the angular coordinate $\phi\,[\mathrm{mod}\,2\pi]$ of $\mathbf{p}$ on the Fermi surface.

We may now consider the collisionless limit of the kinetic equation, Eq. (12), to determine whether undamped zero-sound modes exist. The charge channel in this case gives rise to the usual zero-temperature two-dimensional (2D) plasmon mode, which has been thoroughly studied [4,31–33], and thus we will focus here solely on the charge-neutral modes. Using the parametrization along with the real-space and time Fourier transforms in Eq. (12), we find for the collisionless ($\hat{I}[\delta\hat{\rho}] \to 0$) limit:

$$\omega\nu^\mu(\phi) - v_Fq\cos\phi\times\left[\nu^\mu(\phi) + \frac{G_sG_vp_F}{v_F}\oint d\phi' f^\mu(\phi-\phi')\nu^\mu(\phi')\right] = v_F\mathcal{F}^\mu\cos(\phi-\chi), \tag{16}$$

where v_F is the Fermi velocity, p_F is the Fermi momentum, and ϕ and χ are the angles which the vectors $\mathbf{p}$ and $\boldsymbol{\mathcal{F}}^\mu$ respectively make with $\mathbf{q}$.

We may estimate the Landau-Fermi liquid functions $f^\mu(\mathbf{p}\cdot\mathbf{p}')$ within the Hartree-Fock approximation. Due to the symmetrization of the interaction Hamiltonian one finds

$$f^\mu(\mathbf{p}\cdot\mathbf{p}') \approx 2U^\mu_{\mathbf{p},\mathbf{p}',\mathbf{q}\to0}. \tag{17}$$

Given the hierarchy of energy scales, Eq. (8), the leading contribution to the Fermi-liquid interaction functions comes from the long-ranged function $V(q)$,

$$f^\mu(\theta) \approx -\frac{1}{2}V\left[2k_F\sin\frac{\theta}{2}\right]\times\left[\cos^2\left(\frac{\theta}{2}\right) + \frac{\Delta^2}{(\Delta+E_F)^2}\sin^2\left(\frac{\theta}{2}\right)\right], \tag{18}$$

where $\theta = \phi - \phi'$ is the angle between $\mathbf{p}$ and $\mathbf{p}'$. We note that $f^\mu(\theta) < 0$ at all θ for all neutral modes identified in Eqs. (9). Accounting for the smaller interaction constants identified in Eqs. (7) does not change this conclusion. At $\mathcal{F}^\mu = 0$, we may bring Eq. (16) to the form

$$\widetilde{\nu}^\mu(\phi) = \frac{G_sG_vp_F}{v_F}\oint d\phi' f^\mu(\phi-\phi')\frac{\widetilde{\nu}^\mu(\phi')}{s-\cos\phi'} \tag{19}$$

with $s = \omega/(v_Fq)$ and $\widetilde{\nu}^\mu = (s-\cos\phi)\nu^\mu$. Following the arguments of Ref. [34], we do not expect real-valued solutions with $s > 1$ for $f^\mu < 0$ (one may show that for constant interactions there are no solutions at all when $-1/2 < F_0^\mu < 0$). Therefore, we infer that all neutral modes are overdamped [35], albeit this does not exclude the possibility of a nontrivial response in the time domain [36].

IV. RELAXATION OF SPIN-VALLEY COLLECTIVE MODES

The absence of propagating neutral modes leads us to conclude that at a finite temperature T spreading of an initially localized perturbation in these channels is ultimately controlled by diffusion. In fact, as we will see, neutral first sound modes are not supported and the finite-temperature behavior in these channels is generically diffusive. Next, we evaluate the corresponding diffusion coefficients. For that, we need to find transport scattering times τ^μ_{tr}. These are defined by the linearized collision integral in Eq. (12). For temperatures below the Bloch-Grüneisen temperature $T \ll T_{\mathrm{BG}}$, electron-phonon scattering can be neglected as it will contribute at order T^4 [24,37]. Thus in a clean system, at low temperatures, the collision integral will be dominated by electron-electron collisions which will be seen to contribute at order T^2.

The evaluation of the linearized collision integrals is greatly simplified by a choice of basis for each channel in which the linearized deviation of the density matrix is diagonal. Because of the $SU(2)$ spin and $U(1)$ valley symmetries we need only consider the kinetic equations for s^z, Y_z, M_x^z, and for Y_x, M_z^z. We therefore consider the collision integral in $\sigma_z\tau_z$ and $\sigma_z\tau_x$ bases, respectively. In each of the two, the linearized collision-integral matrix is diagonal and can be written in a familiar form,

$$I(\mathbf{p}_i,\alpha) = -\frac{1}{T}\sum_{\beta\gamma\delta}\sum_{\mathbf{p}_j\mathbf{p}_{i'}\mathbf{p}_{j'}}(2\pi)^2\delta\left(\sum_J{}'\mathbf{p}_J\right) \times 2\pi\delta\left(\sum_J{}'\epsilon_J\right) n_i n_j(1-n_{i'})(1-n_{j'}) \times W_{ij;i'j'}^{\alpha\beta;\gamma\delta}[\bar{\nu}_{i\alpha}+\bar{\nu}_{j\beta}-\bar{\nu}_{i'\gamma}-\bar{\nu}_{j'\delta}], \tag{20}$$

in terms of the reparametrization $\delta\bar{\rho}_{i\alpha}(\mathbf{p},\mathbf{r}) \equiv -(\partial n/\partial\epsilon)\bar{\nu}_{i\alpha}(\phi,\mathbf{r})$ where $\bar{\rho}_{i\alpha} = \bar{\rho}_{\alpha\alpha}(\mathbf{p}_i)$ is the $\alpha = \sigma,\zeta$ component of the *diagonal* deviation, defined analogously to Eq. (14), in the chosen basis. Here we have used the shorthand $\sum_J' h_J$ to denote sums of the form $h_i + h_j - h_{i'} - h_{j'}$, $n_i = n_F(\mathbf{p}_i)$ is the Fermi function at momentum $\mathbf{p}_i$, and W is the square of the amplitude for two particles in states α,β to scatter into states $\gamma\delta$, which may be written in terms of the two-particle t matrix as $W_{ij;ij'}^{\alpha\beta;\gamma\delta} = |\langle i\alpha; j\beta|\hat{t}|i'\gamma; j'\delta\rangle|^2$.

The trace operation on the right-hand side of Eq. (12) is then simply the weighted sum $\mathrm{tr}(\hat{X}^\mu\hat{I}) = \sum_\alpha \lambda_\alpha^\mu I_\alpha$, where λ_α^μ is the eigenvalue corresponding to eigenvector $|\alpha\rangle$ of matrix X^μ. Upon performing the trace the collision integral for each channel can be separated into two parts: those involving scattering of particles with the same quantum number in that channel and those involving scattering of particles with different quantum numbers [e.g., same spin or opposite spin, respectively, for the case of the spin mode; cf. Eq. (22)], which we denote I_+ and I_-, respectively. The former has the same structure as the collision integral for the charge channel and is known in two dimensions to give rise to a transport scattering time which goes as T^4 for low temperatures [38]. The latter term, on the other hand, will be seen to scale as $T^2\ln T$ and comprises the dominant contribution to relaxation of currents in each channel,

$$\mathrm{tr}(\hat{X}^\mu\hat{I}) \to I_-^\mu(\mathbf{p}_i) = -\frac{1}{T}\sum_{\mathbf{p}_j\mathbf{p}_{i'}\mathbf{p}_{j'}}(2\pi)^2\delta\left(\sum_J{}'\mathbf{p}_J\right) \times 2\pi\delta\left(\sum_J{}'\epsilon_J\right) n_i n_j(1-n_{i'})(1-n_{j'}) \times W_-^\mu\left(\bar{\nu}_i^\mu - \bar{\nu}_j^\mu - \bar{\nu}_{i'}^\mu + \bar{\nu}_{j'}^\mu\right), \tag{21}$$

with scattering probabilities

$$\begin{aligned} W_-^s &= 2(W_{\uparrow\downarrow;++}^D + W_{\uparrow\downarrow;+-}^D),\\ W_-^{vz} &= 2(W_{\uparrow\uparrow;+-}^D + W_{\uparrow\downarrow;+-}^D),\\ W_-^{mz} &= 2(W_{\uparrow\uparrow;+-}^D + W_{\uparrow\downarrow;++}^D),\\ W_-^{v\parallel} &= 2(W_{\uparrow\uparrow;+-}^{xD} + W_{\uparrow\downarrow;+-}^{xD}),\\ W_-^{m\parallel} &= 2(W_{\uparrow\uparrow;+-}^{xD} + W_{\uparrow\downarrow;++}^{xD}), \end{aligned} \tag{22}$$

where $W_{\sigma\sigma';\zeta\zeta'}^D$ is the scattering probability for two *distinguishable* particles with spins σ,σ' and valley indices ζ,ζ' and the superscript x indicates the choice of the τ^x eigenbasis in valley space. These may in turn be written in terms of components of the t matrix. In the first Born approximation, this can be expressed in terms of the functions in Eq. (5) as

$$\begin{aligned} W_{\uparrow\downarrow;++}^D &= 4|U_d - U_s + U_{vz} - U_{mz}|^2,\\ W_{\uparrow\downarrow;+-}^D &= 4|U_d - U_s - U_{vz} + U_{mz}|^2,\\ W_{\uparrow\uparrow;+-}^D &= 4|U_d + U_s - U_{vz} - U_{mz}|^2,\\ W_{\uparrow\downarrow;++}^{xD} &= 4|U_d - U_s + U_{v\parallel} - U_{m\parallel}|^2,\\ W_{\uparrow\downarrow;+-}^{xD} &= 4|U_d - U_s - U_{v\parallel} + U_{m\parallel}|^2,\\ W_{\uparrow\uparrow;+-}^{xD} &= 4|U_d + U_s - U_{v\parallel} - U_{m\parallel}|^2. \end{aligned} \tag{23}$$

To the lowest order in T/T_F, the Fermi functions restrict the summation over momenta in Eq. (21) to the states close to the Fermi surface. One may then transform [28,39] the summation to integration over the energies ϵ,ϵ' of the incoming particles, the energy transferred in a collision ω, and the scattering angle θ_{sc}. Due to the constraints on ϵ,ϵ' and conservation laws, the incoming particles collide almost head on, or their momenta are almost collinear to each other. To evaluate the transport relaxation times τ_{tr}^μ, we use $\nu^\mu(\phi)\propto\cos\phi$ [40] to arrive at

$$\frac{1}{\tau_{\mathrm{tr}}^\mu} = \frac{4\nu_F T^2}{v_F^2}\int d\Sigma\int_0^{\pi-\theta_c}\frac{d\theta_{\mathrm{sc}}}{\sin\theta_{\mathrm{sc}}}(1-\cos\theta_{\mathrm{sc}}) \times\left(W_{-,\mathrm{collinear}}^\mu(\theta_{\mathrm{sc}}) + W_{-,\mathrm{head\text{-}on}}^\mu(\theta_{\mathrm{sc}})\right). \tag{24}$$

The logarithmic divergence [41] at $\theta_{\mathrm{sc}} = \pi$ is cut off by $\theta_c \sim T/E_F$ due to the kinematic constraints on scattering of particles on the Fermi surface (see Appendix C 1 for details). For compactness, we have defined the dimensionless energy integration measure

$$d\Sigma = \frac{1}{4\pi^2}dudu'dwn_i n_j(1-n_{i'})(1-n_{j'}) \tag{25}$$

in terms of dimensionless variables $u = \epsilon/T$, $w = \omega/T$, $\epsilon_i,\epsilon_{i'} = \epsilon \pm \omega/2$, and $\epsilon_j,\epsilon_{j'} = \epsilon' \mp \omega/2$. In the case where $q_{\mathrm{TF}} \ll 2k_F$ there is also a logarithmic contribution due to collinear scattering by the Coulomb potential, which is cut off by the Thomas-Fermi wavenumber q_{TF} [42–44]. In graphene, unlike more conventional Fermi liquids, $q_{\mathrm{TF}} = G_s G_V \alpha v k_F/v_F$ can be greater than $2k_F$ due to the degeneracy factors and strong effective coupling $\alpha = e^2/\kappa v$. In this complementary regime, the collinear scattering logarithm is absent and the dominant matrix element for backscattering will be screened. We present here explicit expressions for the former case, $q_{\mathrm{TF}} \ll 2k_F$, but one may straightforwardly perform the analogous calculations in the latter case and the qualitative results remain the same. Which regime is realized experimentally will depend on the background dielectric constant and doping.

Thus, performing the integration in Eq. (24), with $q_{\rm TF} \ll 2k_F$, we find

$$\frac{1}{\tau_{\rm tr}^{\mu}(T)} = \frac{4\pi}{3}(E_F+\Delta)\alpha^2\frac{T^2}{E_F^2}\left(\frac{1+E_F/\Delta}{1+E_F/2\Delta}\right)^2\left\{\left(\frac{\Delta}{\Delta+E_F}\right)^4 \times \ln\frac{\sqrt{E_F(E_F+2\Delta)}}{T} + \ln\frac{\sqrt{E_F(E_F+2\Delta)}}{v q_{\rm TF}}\right\} \quad (26)$$

in the leading logarithmic approximation, applicable at $T \ll \sqrt{E_F\Delta}$. In the evaluation of the scattering probabilities entering Eq. (24), we used the Born approximation and the Thomas-Fermi screened Coulomb potential [cf. Eqs. (8) and (23)]. The first logarithmic contribution in Eq. (26) comes from the backscattering amplitude ($\theta_{\rm sc} = \pi$), as long as it remains finite. Notably, backscattering is suppressed in graphene at $\Delta \ll E_F$ due to the presence of the Berry phase in the electron eigenfunctions [23,24]. Therefore, in the relativistic limit $\Delta \to 0$, Eq. (26) is replaced by (see Appendix D)

$$\frac{1}{\tau_{\rm tr}^{\mu}(T)} = \frac{4}{3\pi}\frac{T^2}{E_F^2}\left\{N_\mu\left(g_\mu\frac{E_F}{v_F}\right)^2\ln\frac{E_F}{T} + (2\pi\alpha)^2 E_F\ln\frac{E_F}{v q_{\rm TF}}\right\}. \quad (27)$$

Here $g_\mu = g_{\perp\perp}$ for $\mu = vz, mz, v\parallel, m\parallel$, and $g_\mu = g_{zz}$ for $\mu = s$, and the numerical factor $N_\mu = 8$ for $\mu = vz, mz$, $N_\mu = 10$ for $\mu = v\parallel, m\parallel$, and $N_\mu = 4$ for $\mu = s$. We note that the logarithmic terms associated with the backscattering in Eq. (27) generically are smaller than those present at $\Delta \sim E_F$ [cf. Eqs. (7), (8), and (26)]. The diffusion constant for each of the channels is $D_\mu = v_F^2\tau_{\rm tr}^{\mu}/2$ (consistent with the Born approximation, here we dispensed with the Fermi liquid correction [28,34] to the Fermi velocity). The diffusion regime settles in at times $t \gtrsim \tau_{\rm tr}(T)$.

V. DISCUSSION

The relaxation rates for the neutral modes can be experimentally probed through nonlocal resistance measurements using the spin and valley Hall effects [29,45,46]. Currently experimental measurements of spin and valley diffusion below the Bloch-Grüneisen temperature have obtained diffusion constants corresponding to mean free paths of the order 0.1 μm [46–49]. Calculations performed in the limit $q_{\rm TF} \ll k_F$ give significantly longer mean free paths, indicating either that impurities play the dominant role, or the system is in the regime $k_F \ll q_{\rm TF}$. Nonetheless, experimental works on electron hydrodynamics suggest that it could be possible to reach the regime where electron-electron effects dominate the response of the neutral modes [7–11], as considered here. Thus, the predicted relaxation rates—and their temperature dependence—should be measurable, either via the same types of experiments as have been previously used to measure spin and valley diffusion, or through other methods [50].

The generalization of Eq. (24) to higher angular harmonics ($m \geqslant 2$) of the distribution function $\nu(\phi)$ is presented in Appendix C. The relaxation rate $1/\tau_2(T)$ of the $m = 2$ harmonic is similar to $1/\tau_{\rm tr}(T)$ of Eqs. (26) and (27) and is likely lower than $1/\tau_{\rm tr}(T)$ in the respective limits, as $1/\tau_2(T)$ lacks the logarithmic enhancement of the backscattering contribution.

The hierarchy $\tau_{\rm tr} \lesssim \tau_2$ for all of the graphene Fermi liquid neutral modes excludes the possibility of a hydrodynamic sound mode, contrary to the case of the density mode in a conventional neutral Fermi liquid (for the density mode, $1/\tau_{\rm tr} \equiv 0$ by translation invariance). Combined with the discussion below Eq. (19), we thus find that both zero and first sound are absent in *all neutral channels*.

Relaxation of the higher-m moments of the distribution function can be measured in magnetic focusing experiments [51]. With the increase of m, the role of the forward-scattering contribution [which gave rise to the second term in Eqs. (26) and (27)] strengthens. At $m \gg 2k_F/q_{\rm TF}$ and sufficiently low temperatures the small-angle scattering involving the screened Coulomb potential $V(0) = 1/(G_s G_v[1+F_0^d])$ dominates the relaxation rate $1/\tau_m \sim (T^2/vk_F)\ln m$. The asymptotic large-$m$ relaxation of spin modes can then be accessed in focusing experiments utilizing spin-polarized leads in a setup similar to that of Ref. [51].

In the above we have assumed $SU(2)$ spin invariance, leading to diffusion of the conserved spin density as described by Eqs. (26) and (27). Spin-orbit coupling destroys the $SU(2)$ symmetry and leads to the interaction-induced relaxation of a net spin polarization. An expression for the associated relaxation rate was obtained by Glazov and Ivchenko [52] in terms of the spin-orbit coupling strength and electron-electron collision rates [53]. We neglect such a combined effect here as intrinsic spin-orbit coupling in graphene is weak [12], but in the presence of extrinsic spin-orbit coupling [54] similar relaxation effects would be expected for the spin-valley channels studied in this work.

Throughout this work we disregarded the trigonal warping of the electron spectrum in graphene. Warping does not destroy the used $U(2)\times U(2)$ spin-valley symmetries. The modification of the spectrum, however, cuts off the logarithmic singularity of backscattering in Eq. (24) and introduces anisotropy of the diffusion coefficient due to the dependence of the Fermi velocity on the direction of the electron wave vector. For similar reasons, the calculations presented herein may be extended to twisted bilayer graphene, which also possesses an internal $U(2)\times U(2)$ symmetry [55,56], and thus at a generic filling we also expect similar qualitative behavior such as the absence of neutral zero or first sound, and a transport scattering time for the neutral modes which scales as $(W/T)^2\ln W/T$ where W is the bandwidth of the nearly flat bands. As the flat-band limit is approached one must consider both the valence and conduction bands together and modes associated with the interband transitions will appear which could exhibit different behaviors given the enlarged symmetry $U(4)$ [$U(4)\times U(4)$ for the chiral case] [55,56] of the flat-band limit.

ACKNOWLEDGMENTS

The authors would like to thank M. Kharitonov and I. Aleiner. Z.M.R. would also like to thank J. Wilson for helpful discussions. This work was supported by NSF Grant No. DMR-2002275 (L.I.G.), European Graphene Flagship Core 3 Project, Lloyd Register Foundation Nanotechnology Grant, EPSRC Grants No. EP/S030719/1 and No. EP/N010345/1 (V.I.F.), and the Yale Prize Postdoctoral Fellowship in Condensed Matter Theory (Z.M.R.).

TABLE I. Transformation properties of short-range interaction vertices, grouped by whether they are even or odd under time reversal θ and mirror plane σ_V.

	θ even	θ odd
σ_v even	$\Sigma_y\tau_y$, $\Sigma_x\tau_z$, $\Sigma_x\tau_x$, $\Sigma_z\tau_x$, $\Sigma_z\tau_z$	Σ_y, τ_y
σ_v odd	$\Sigma_y\tau_x$, $\Sigma_y\tau_z$, $\Sigma_x\tau_y$, $\Sigma_z\tau_y$	Σ_x, Σ_z, τ_x, τ_z

APPENDIX A: SYMMETRY-IMPOSED FORM OF THE INTERACTION FUNCTIONS

In this section we derive the short-ranged interaction terms which are consistent with the symmetry of the gapped graphene lattice and relate them to the interaction functions in the spin-valley channels introduced in Eq. (5).

1. Symmetry analysis of short-ranged interactions

Ignoring out-of-plane behavior, the point group of gapped graphene is C_{3v}. In the absence of spin-orbit coupling, which is generally weak in graphene, the local symmetry is enlarged to $C_{3V} \oplus SU(2)$. In the valley-sublattice basis with spinor

$$\Psi_{\mathbf{k}} = \begin{pmatrix} \psi_{KA}(\mathbf{k}) \\ \psi_{KB}(\mathbf{k}) \\ \psi_{K'B}(\mathbf{k}) \\ -\psi_{K'A}(\mathbf{k}) \end{pmatrix} \tag{A1}$$

we can define the representative symmetry operators

$$C_3 : e^{i\frac{\pi}{3}\hat{\Sigma}_3}, \quad \sigma_V : \hat{\Sigma}_2\hat{\tau}_2, \quad \Theta : \sigma_V K, \quad T : e^{\frac{2\pi i}{3}\tau^z}, \tag{A2}$$

describing, respectively, C_3 rotation, mirror plane, time reversal, and lattice translation. Here Σ, σ, and τ denote sublattice, spin, and valley Pauli matrices, respectively. Doing so we classify the bilinears of matrices which form invariants under the symmetry group. We note that s_x, s_y and τ_x, τ_y form doublets under C_3 and T, respectively. We may now tabulate which matrices are even or odd under σ_V and θ in Table I. Combining all this we find that the symmetry-allowed short-range interactions are

$$\begin{gathered} \mathbb{1}^1\cdot\mathbb{1}^2,\ \boldsymbol{\Sigma}^1_\parallel\cdot\boldsymbol{\Sigma}^2_\parallel,\ \boldsymbol{\tau}^1_\parallel\cdot\boldsymbol{\tau}^2_\parallel,\ \Sigma^1_z\Sigma^2_z,\ \tau^1_z\tau^2_z, \\ \boldsymbol{\Sigma}^1_\parallel\cdot\boldsymbol{\Sigma}^2_\parallel\boldsymbol{\tau}^1_\parallel\cdot\boldsymbol{\tau}^2_\parallel,\ \boldsymbol{\Sigma}^1_\parallel\cdot\boldsymbol{\Sigma}^2_\parallel\tau^1_z\tau^2_z,\ \boldsymbol{\tau}^1_\parallel\cdot\boldsymbol{\tau}^2_\parallel\Sigma^1_z\Sigma^2_z, \\ \Sigma^1_z\tau^1_z\Sigma^2_z\tau^2_z,\ \Sigma^1_z\cdot\tau^2_z,\ \Sigma^1_z\tau^1_z\cdot\mathbb{1}^2, \end{gathered} \tag{A3}$$

where we use the superscripts 1 and 2 to indicate that the vertex is for particle 1 or 2, respectively. We can estimate the interaction constants for these channels by inserting the Dirac cone ansatz for the creation operator,

$$\begin{aligned} \Psi = {} & u_{KA}\psi_{KA} + u_{KB}\psi_{KB} \\ & + u_{K'B}\psi_{K'B} + u_{K'A}\psi_{K'A}, \end{aligned} \tag{A4}$$

into the Coulomb interaction. Because of the relations

$$u_{KA} = u^*_{K'A}, \quad u_{KB} = u^*_{K'B}, \tag{A5}$$

the vertices which are odd under time reversal vanish. The remaining vertices are

$$\begin{gathered} \mathbb{1}^1\cdot\mathbb{1}^2,\ \boldsymbol{\Sigma}^1_\parallel\cdot\boldsymbol{\Sigma}^2_\parallel\boldsymbol{\tau}^1_\parallel\cdot\boldsymbol{\tau}^2_\parallel,\ \boldsymbol{\Sigma}^1_\parallel\cdot\boldsymbol{\Sigma}^2_\parallel\tau^1_z\tau^2_z, \\ \boldsymbol{\tau}^1_\parallel\cdot\boldsymbol{\tau}^2_\parallel\Sigma^1_z\Sigma^2_z,\ \Sigma^1_z\tau^1_z\Sigma^2_z\tau^2_z,\ \Sigma^1_z\tau^1_z\cdot\mathbb{1}^2_z, \end{gathered} \tag{A6}$$

to which we assign, respectively, the coupling constants

$$g_{00},\ g_{\perp\perp},\ g_{z\perp},\ g_{\perp z},\ g_{zz},\ \tilde{g}_{00}. \tag{A7}$$

Neglecting the overlap of the A and B sublattice Bloch wavefunctions we can further discard the $g_{z\perp}, g_{\perp z}$ terms and we arrive at

$$\begin{aligned} \hat{H}^{\psi}_{\text{int}} = {} & \frac{1}{2}\sum_{\mathbf{r},\mathbf{r}'} V(\mathbf{r}-\mathbf{r}') :\psi^\dagger(\mathbf{r})\psi(\mathbf{r})\psi^\dagger(\mathbf{r}')\psi(\mathbf{r}'): \\ & + \frac{1}{2}\sum_{\mathbf{r}}\sum_{\alpha\beta}[g_{\alpha\beta}:\psi^\dagger(\mathbf{r})\Sigma^\alpha\tau^\beta\psi(\mathbf{r})\psi^\dagger(\mathbf{r}')\Sigma^\alpha\tau^\beta\psi(\mathbf{r}'): \\ & + \tilde{g}_{00}:\psi^\dagger(\mathbf{r})\Sigma^z\tau^z\psi(\mathbf{r})\psi^\dagger(\mathbf{r}')\psi(\mathbf{r}'):]. \end{aligned} \tag{A8}$$

2. Interaction functions in terms of short-ranged interaction constants

Writing the fermionic annihilation operator

$$\hat{\Psi}_\sigma(\mathbf{r}) = u_{KA}(\mathbf{r})\, u_{KB}(\mathbf{r})\, u_{K'B}(\mathbf{r})\ - u_{K'A}(\mathbf{r})\cdot\hat{\vec{\psi}}_\sigma(\mathbf{r}), \tag{A9}$$

the upper band projected operator has the form $\vec{\psi}_{\mathbf{k}\sigma} = \sum_\zeta \chi_{\mathbf{k}\zeta}c_{\mathbf{k}\zeta\sigma}$, where

$$\chi_{\mathbf{k}+} = \begin{pmatrix} \sqrt{\frac{1}{2}\left(1+\frac{\Delta}{E_{\mathbf{k}}}\right)} \\ e^{i\phi_{\mathbf{k}}}\sqrt{\frac{1}{2}\left(1-\frac{\Delta}{E_{\mathbf{k}}}\right)} \end{pmatrix}, \quad \chi_{\mathbf{k}-} = -\begin{pmatrix} e^{-i\phi_{\mathbf{k}}}\sqrt{\frac{1}{2}\left(1-\frac{\Delta}{E_{\mathbf{k}}}\right)} \\ \sqrt{\frac{1}{2}\left(1+\frac{\Delta}{E_{\mathbf{k}}}\right)} \end{pmatrix}. \tag{A10}$$

By plugging the upper band operator into Eq. (6), the interaction functions in Eq. (5) can then be expressed in terms of the interaction constants $g_{zz}, g_{\perp\perp}, \widetilde{g}_{00}$ and the function $V(\mathbf{q})$ combined with matrix elements of the eigenspinors $\chi_{\mathbf{k}\zeta}$. Using the shorthand

$$\begin{aligned} F_{ij;i'j'} & \equiv F(\mathbf{p}_i, \mathbf{p}_j; \mathbf{p}_{i'}, \mathbf{p}_{j'}) \\ & \equiv F(\mathbf{p}+\mathbf{q}/2, \mathbf{p}' \\ & \quad -\mathbf{q}/2; \mathbf{p}-\mathbf{q}/2, \mathbf{p}'+\mathbf{q}/2), \end{aligned} \tag{A11}$$

we can write

$$U^d_{\mathbf{p},\mathbf{p}',\mathbf{q}} = \tfrac{1}{2}\big(V_{\mathbf{q}}L_{ii'}L_{jj'} - \tfrac{1}{4}V_{\mathbf{p}-\mathbf{p}'}L_{ij'}L_{ji'} + g_{zz}\big(N_{ii'}N_{jj'} - \tfrac{1}{4}N_{ij'}N_{ji'}\big)\tfrac{1}{2}\tilde{g}_{00}\big(Q^{00}_{ii';jj'} - \tfrac{1}{4}Q^{00}_{ij';ji'}\big) - \tfrac{1}{2}g_{\perp\perp}Q^{\perp\perp}_{ij';ji'}\big),$$

$$U^s_{\mathbf{p},\mathbf{p}',\mathbf{q}} = -\tfrac{1}{4}\big(\tfrac{1}{2}V_{\mathbf{p}-\mathbf{p}'}L_{ij'}L_{ji'} + \tfrac{1}{2}g_{zz}N_{ij'}N_{ji'} + \tfrac{1}{4}\tilde{g}_{00}Q^{00}_{ij';ji'} + g_{\perp\perp}Q^{\perp\perp}_{ij';ji'}\big),$$

$$U^{v\parallel}_{\mathbf{p},\mathbf{p}',\mathbf{q}} = -\tfrac{1}{2}\big(\tfrac{1}{4}V_{\mathbf{p}-\mathbf{p}'}L_{ij'}L_{ji'} + \tfrac{1}{4}g_{zz}N_{ij'}N_{ji'} + \tfrac{1}{8}\tilde{g}_{00}Q^{00}_{ij';ji'} - g_{\perp\perp}Q^{\perp\perp}_{ii';jj'}\big),$$

$$U^{vz/mz}_{\mathbf{p},\mathbf{p}',\mathbf{q}} = -\tfrac{1}{4}\big(\tfrac{1}{2}V_{\mathbf{p}-\mathbf{p}'}L_{ij'}L_{ji'} + \tfrac{1}{2}g_{zz}N_{ij'}N_{ji'} + \tfrac{1}{4}\tilde{g}_{00}Q^{00}_{ij';ji'} - g_{\perp\perp}Q^{\perp\perp}_{ij';ji'}\big),$$
$$U^{m\parallel}_{\mathbf{p},\mathbf{p}',\mathbf{q}} = -\tfrac{1}{8}\big(V_{\mathbf{p}-\mathbf{p}'}L_{ij'}L_{ji'} + g_{zz}N_{ij'}N_{ji'} + \tfrac{1}{2}\tilde{g}_{00}Q^{00}_{ij';ji'}\big), \tag{A12}$$

where

$$Q^{\perp\perp}_{ii';jj'} = \tilde{L}_{ii'}\tilde{L}^*_{jj'} + \tilde{N}_{ii'}\tilde{N}^*_{jj'}, Q^{00}_{ii';jj'} = L_{ii'}N_{jj'} + N_{ii'}L_{jj'},$$
$$L(\mathbf{k},\mathbf{k}') = \chi^\dagger_{\mathbf{k}+}\chi_{\mathbf{k}'+},\ N(\mathbf{k},\mathbf{k}') = \chi^\dagger_{\mathbf{k}+}\tau_3\chi_{\mathbf{k}'+},$$
$$\tilde{L}(\mathbf{k},\mathbf{k}') = \chi^\dagger_{\mathbf{k}+}\chi^*_{\mathbf{k}'+}, \tilde{N}(\mathbf{k},\mathbf{k}') = \chi^\dagger_{\mathbf{k}+}\tau_3\chi^*_{\mathbf{k}'+}. \tag{A13}$$

Of particular note are the limits of the coherence factors L, N, $\tilde{L}$, and $\tilde{N}$,

$$L(\mathbf{k},\mathbf{k}) = N(\mathbf{k},-\mathbf{k}) = 1,\ \ L(\mathbf{k},-\mathbf{k}) = N(\mathbf{k},\mathbf{k}) = \frac{\Delta}{E_{\mathbf{k}}}, \tag{A14}$$

where the latter relation is responsible for the suppression of backscattering in the relativistic, $\Delta \to 0$ limit.

APPENDIX B: LOW-ENERGY INTERACTIONS FROM THE COULOMB INTERACTION

In this section, we estimate the strength of short-range interactions in the various spin-valley channels.

We can obtain estimates for the interaction strengths occurring in Eqs. (6) and (A12) by looking at the matrix elements of the Coulomb interaction. In particular we aim to obtain the lowest harmonic of the Coulomb interaction contributing to each interaction strength above.

We begin by writing the interaction Hamiltonian for the physical electrons in the bands nearest the Fermi surface:

$$\hat{H}_{\text{int}} = \frac{1}{2}\sum_{\lambda\lambda',\sigma\sigma'}\int d\mathbf{r}d\mathbf{r}' V(|\mathbf{r}-\mathbf{r}'|) \times :c^\dagger_{\sigma\lambda}(\mathbf{r})c_{\sigma\lambda}(\mathbf{r})c^\dagger_{\sigma'\lambda'}(\mathbf{r}')c_{\sigma'\lambda'}(\mathbf{r}'):, \tag{B1}$$

where σ denotes spin, $\lambda = \pm 1$ denotes the sublattice A and B states, respectively, $:\cdots:$ denotes normal ordering, and $V(|\mathbf{R}|)$ is the Coulomb interaction. The operators may be expanded in terms of Bloch states,

$$c_{\sigma\lambda}(\mathbf{r}) = \int_{\text{BZ}}\frac{d\mathbf{p}}{(2\pi)^2}\psi_{\lambda\mathbf{p}}(\mathbf{r})c_{\sigma\lambda}(\mathbf{p}), \tag{B2}$$

with wavefunction

$$\psi_{\lambda\mathbf{p}}(\mathbf{r}) = e^{i\mathbf{p}\cdot\mathbf{r}}u_{\lambda\mathbf{p}}(\mathbf{r}). \tag{B3}$$

Using the Bloch basis and the Fourier transform of the Coulomb interaction we can rewrite Eq. (B1):

$$\hat{H}_{\text{int}} = \frac{1}{2}\sum_{\lambda\lambda',\sigma\sigma'}\int_{\text{BZ}}\left[\prod_i\frac{d\mathbf{p}_i}{(2\pi)^2}\right]\int_{\mathbb{R}^2}\frac{d\mathbf{q}}{(2\pi)^2} \times V(q):c^\dagger_{\sigma\lambda}(\mathbf{p}_1)c_{\sigma\lambda}(\mathbf{p}'_1)c^\dagger_{\sigma'\lambda'}(\mathbf{p}_2)c_{\sigma'\lambda'}(\mathbf{p}'_2): \times\int_{\mathbb{R}^2}d\mathbf{r}d\mathbf{r}'e^{i\mathbf{q}\cdot(\mathbf{r}-\mathbf{r}')} \times\psi^*_{\lambda\mathbf{p}_1}(\mathbf{r})\psi_{\lambda\mathbf{p}'_1}(\mathbf{r})\psi^*_{\lambda\mathbf{p}_2}(\mathbf{r}')\psi_{\lambda\mathbf{p}'_2}(\mathbf{r}'). \tag{B4}$$

We can rewrite the integral of $\mathbf{q}$ as an integral over the Brillouin zone and a sum over all reciprocal lattice vectors,

$$\int_{\mathbb{R}^2}\frac{d\mathbf{q}}{(2\pi)^2}f(\mathbf{q}) = \sum_{\mathbf{G}}\int_{\text{BZ}}\frac{d\mathbf{q}}{(2\pi)^2}f(\mathbf{q}+\mathbf{G}), \tag{B5}$$

where we have introduced the shorthand

$$\sum_{\mathbf{G}}f(\mathbf{G}) \equiv \sum_{n_1,n_2}f(n_1\mathbf{b}_1 + n_2\mathbf{b}_2) \tag{B6}$$

with $\mathbf{b}_i$ the primitive reciprocal lattice vectors. Similarly we can rewrite the integration over all space in terms of integration over the unit cell,

$$\int_{\mathbf{R}^2}d\mathbf{r}f(\mathbf{r}) = \sum_{\mathbf{R}}\int_{\text{uc}}d\mathbf{r}f(\mathbf{r}+\mathbf{R}), \tag{B7}$$

where we have analogously defined the shorthand

$$\sum_{\mathbf{R}}f(\mathbf{R}) \equiv \sum_{n_1,n_2}f(n_1\mathbf{a}_1 + n_2\mathbf{a}_2) \tag{B8}$$

with $\mathbf{a}_i$ the primitive translation vectors of the lattice. Using both these relations, the interaction Hamiltonian becomes

$$\hat{H}_{\text{int}} = \frac{1}{2}\sum_{\lambda\lambda',\sigma\sigma'}\sum_{\mathbf{G}}\int_{\text{BZ}}\left[\prod_i\frac{\mathbf{p}_i}{(2\pi)^2}\right]\int_{\text{BZ}} \times\frac{d\mathbf{q}}{(2\pi)^2}:c^\dagger_{\sigma\lambda}(\mathbf{p}_1)c_{\sigma\lambda}(\mathbf{p}'_1)c^\dagger_{\sigma'\lambda'}(\mathbf{p}_2)c_{\sigma'\lambda'}(\mathbf{p}'_2): \times V(|\mathbf{q}+\mathbf{G}|)\sum_{\mathbf{R},\mathbf{R}'}e^{i\mathbf{q}\cdot(\mathbf{R}-\mathbf{R}')}e^{-i(\mathbf{p}_1-\mathbf{p}'_1)\cdot\mathbf{R}}e^{-i(\mathbf{p}_2-\mathbf{p}'_2)\cdot\mathbf{R}'} \times\int_{\text{uc}}d\mathbf{r}d\mathbf{r}'e^{i(\mathbf{q}+\mathbf{G})\cdot(\mathbf{r}-\mathbf{r}')}\psi^*_{\lambda\mathbf{p}_1}(\mathbf{r})\psi_{\lambda\mathbf{p}'_1}(\mathbf{r}) \times\psi^*_{\lambda\mathbf{p}_2}(\mathbf{r}')\psi_{\lambda\mathbf{p}'_2}(\mathbf{r}'), \tag{B9}$$

where we have used $\exp(i\mathbf{G}\cdot\mathbf{R}) = 1$, and the periodicity properties of the Bloch wavefunctions. The sums over $\mathbf{R}, \mathbf{R}'$ can be performed to obtain

$$(2\pi)^2\delta_{\text{BZ}}(\mathbf{p}_1 - \mathbf{p}'_1 - \mathbf{q})(2\pi)^2\delta_{\text{BZ}}(\mathbf{p}_2 - \mathbf{p}'_2 + \mathbf{q}), \tag{B10}$$

where δ_{BZ} is to be resolved modulo the Brillouin zone, as the integrand is periodic in all $\mathbf{p}_i$. We then obtain

$$\hat{H}_{\mathrm{int}} = \frac{1}{2}\sum_{\lambda\lambda',\sigma\sigma'}\sum_{\mathbf{G}}\int_{\mathrm{BZ}}\frac{d\mathbf{p}}{(2\pi)^2}\frac{d\mathbf{p}'}{(2\pi)^2}\int_{\mathrm{BZ}}\frac{d\mathbf{q}}{(2\pi)^2} : c^{\dagger}_{\sigma\lambda}(\mathbf{p}+\mathbf{q})c_{\sigma\lambda}(\mathbf{p})c^{\dagger}_{\sigma'\lambda'}(\mathbf{p}'-\mathbf{q})c_{\sigma'\lambda'}(\mathbf{p}') :$$
$$\times V(|\mathbf{q}+\mathbf{G}|)\int_{\mathrm{uc}} d\mathbf{r}d\mathbf{r}' e^{i(\mathbf{q}+\mathbf{G})\cdot(\mathbf{r}-\mathbf{r}')}\psi^{*}_{\lambda\mathbf{p}+\mathbf{q}}(\mathbf{r})\psi_{\lambda\mathbf{p}}(\mathbf{r})\psi^{*}_{\lambda\mathbf{p}'-\mathbf{q}}(\mathbf{r}')\psi_{\lambda\mathbf{p}'}(\mathbf{r}'), \tag{B11}$$

and in terms of the Bloch factors

$$\hat{H}_{\mathrm{int}} = \frac{1}{2}\sum_{\lambda\lambda',\sigma\sigma'}\sum_{\mathbf{G}}\int_{\mathrm{BZ}}\frac{d\mathbf{p}}{(2\pi)^2}\frac{d\mathbf{p}'}{(2\pi)^2}\int_{\mathrm{BZ}}\frac{d\mathbf{q}}{(2\pi)^2} : c^{\dagger}_{\sigma\lambda}(\mathbf{p}+\mathbf{q})c_{\sigma\lambda}(\mathbf{p})c^{\dagger}_{\sigma'\lambda'}(\mathbf{p}'-\mathbf{q})c_{\sigma'\lambda'}(\mathbf{p}') :$$
$$\times V(|\mathbf{q}+\mathbf{G}|)\int_{\mathrm{uc}} d\mathbf{r}d\mathbf{r}' e^{i\mathbf{G}\cdot(\mathbf{r}-\mathbf{r}')}u^{*}_{\lambda\mathbf{p}+\mathbf{q}}(\mathbf{r})u_{\lambda\mathbf{p}}(\mathbf{r})u^{*}_{\lambda\mathbf{p}'-\mathbf{q}}(\mathbf{r}')u_{\lambda\mathbf{p}'}(\mathbf{r}'). \tag{B12}$$

We may thus write the interaction as

$$\hat{H}_{\mathrm{int}} = \frac{1}{2}\sum_{\lambda\lambda',\sigma\sigma'}\int_{\mathrm{BZ}}\frac{d\mathbf{p}}{(2\pi)^2}\frac{d\mathbf{p}'}{(2\pi)^2}\int_{\mathrm{BZ}}\frac{d\mathbf{q}}{(2\pi)^2}U_{\lambda\lambda'}(\mathbf{p},\mathbf{p}',\mathbf{q}) : c^{\dagger}_{\sigma\lambda}(\mathbf{p}+\mathbf{q})c_{\sigma\lambda}(\mathbf{p})c^{\dagger}_{\sigma'\lambda'}(\mathbf{p}'-\mathbf{q})c_{\sigma'\lambda'}(\mathbf{p}') :, \tag{B13}$$

where we have defined

$$U_{\lambda\lambda'}(\mathbf{p},\mathbf{p}',\mathbf{q}) \equiv \sum_{\mathbf{G}} V(|\mathbf{q}+\mathbf{G}|)\int_{\mathrm{uc}} d\mathbf{r}d\mathbf{r}' e^{i\mathbf{G}\cdot(\mathbf{r}-\mathbf{r}')}u^{*}_{\lambda\mathbf{p}+\mathbf{q}}(\mathbf{r})u_{\lambda\mathbf{p}}(\mathbf{r})u^{*}_{\lambda\mathbf{p}'-\mathbf{q}}(\mathbf{r}')u_{\lambda\mathbf{p}'}(\mathbf{r}'). \tag{B14}$$

Now we make the Dirac cone approximation. We restrict the momenta of each of the electron operators to be in the vicinity of the $\mathbf{K}$ or $\mathbf{K}'$ point. Each of the Bloch factors will be evaluated at the corresponding point. Introducing the notation

$$\int_{\Lambda}\frac{d\mathbf{p}}{(2\pi)^2}\cdots \tag{B15}$$

for integration over momenta $\mathbf{p} \ll |\mathbf{K}-\mathbf{K}'|$ and the operators

$$c_{\sigma\lambda\zeta}(\mathbf{p}) = c_{\sigma\lambda}(\zeta\mathbf{K}+\mathbf{p}) \tag{B16}$$

with $\zeta = \pm 1$ indexing the valley degree of freedom, we may approximate the interaction Hamiltonian as

$$\hat{H}_{\mathrm{int}} \approx \frac{1}{2}\sum_{\lambda\lambda',\sigma\sigma',\zeta_i}\int_{\Lambda}\frac{d\mathbf{p}}{(2\pi)^2}\frac{d\mathbf{p}'}{(2\pi)^2}\int_{\Lambda}\frac{d\mathbf{q}}{(2\pi)^2}U_{\lambda\lambda';\zeta_i}(\mathbf{q}) : c^{\dagger}_{\sigma\lambda\zeta_1}(\mathbf{p}+\mathbf{q})c_{\sigma\lambda\zeta_1'}(\mathbf{p})c^{\dagger}_{\sigma'\lambda'\zeta_2}(\mathbf{p}'-\mathbf{q})c_{\sigma'\lambda'\zeta_2'}(\mathbf{p}') : \tag{B17}$$

with

$$U_{\lambda\lambda';\zeta_i}(\mathbf{q}) \equiv \sum_{\mathbf{G}} V(|\mathbf{q}+\mathbf{G}+(\zeta_1-\zeta_1')\mathbf{K}|)\delta_{\zeta_1-\zeta_1',\zeta_2'-\zeta_2}\int_{\mathrm{uc}} d\mathbf{r}d\mathbf{r}' e^{i\mathbf{G}\cdot(\mathbf{r}-\mathbf{r}')}u^{*}_{\lambda\zeta_1}(\mathbf{r})u_{\lambda\zeta_1'}(\mathbf{r})u^{*}_{\lambda\zeta_2}(\mathbf{r}')u_{\lambda\zeta_2'}(\mathbf{r}'). \tag{B18}$$

There are two types of terms, $\zeta_1 = \zeta_1' = \zeta$, $\zeta_2 = \zeta_2' = \zeta'$ and $\zeta_1 = -\zeta_1' = \zeta_2' = -\zeta_2 = \zeta$. We therefore write

$$\hat{H}_{\mathrm{int}} \approx \frac{1}{2}\sum_{\lambda\lambda',\sigma\sigma',\zeta\zeta'}\int_{\Lambda}\frac{d\mathbf{p}}{(2\pi)^2}\frac{d\mathbf{p}'}{(2\pi)^2}\int_{\Lambda}\frac{d\mathbf{q}}{(2\pi)^2}U^{\mathrm{intra}}_{\lambda\lambda'}(\mathbf{q}) : c^{\dagger}_{\sigma\lambda\zeta}(\mathbf{p}+\mathbf{q})c_{\sigma\lambda\zeta}(\mathbf{p})c^{\dagger}_{\sigma'\lambda'\zeta'}(\mathbf{p}'-\mathbf{q})c_{\sigma'\lambda'\zeta'}(\mathbf{p}') :$$
$$+\frac{1}{2}\sum_{\lambda\lambda',\sigma\sigma',\zeta}\int_{\Lambda}\frac{d\mathbf{p}}{(2\pi)^2}\frac{d\mathbf{p}'}{(2\pi)^2}\int_{\Lambda}\frac{d\mathbf{q}}{(2\pi)^2}U^{\mathrm{inter}}_{\lambda\lambda';\zeta}(\mathbf{q}) : c^{\dagger}_{\sigma\lambda\zeta}(\mathbf{p}+\mathbf{q})c_{\sigma\lambda,-\zeta}(\mathbf{p})c^{\dagger}_{\sigma'\lambda',-\zeta}(\mathbf{p}'-\mathbf{q})c_{\sigma'\lambda'\zeta}(\mathbf{p}') : \tag{B19}$$

with

$$U^{\mathrm{intra}}_{\lambda\lambda'}(\mathbf{q}) \equiv \sum_{\mathbf{G}} V(|\mathbf{q}+\mathbf{G}|)\int_{\mathrm{uc}} d\mathbf{r}d\mathbf{r}' e^{i\mathbf{G}\cdot(\mathbf{r}-\mathbf{r}')}|u_{\lambda+}(\mathbf{r})|^2|u_{\lambda+}(\mathbf{r}')|^2, \tag{B20}$$

where we have used that fact that $u_- = u_+^* \Rightarrow |u_+|^2 = |u_-|^2$ and

$$U^{\mathrm{inter}}_{\lambda\lambda';\zeta}(\mathbf{q}) \equiv \sum_{\mathbf{G}} V(|\mathbf{q}+\mathbf{G}+2\zeta\mathbf{K}|)\int_{\mathrm{uc}} d\mathbf{r}d\mathbf{r}' e^{i\mathbf{G}\cdot(\mathbf{r}-\mathbf{r}')}u^{*}_{\lambda\zeta}(\mathbf{r})u_{\lambda,-\zeta}(\mathbf{r})u^{*}_{\lambda,-\zeta}(\mathbf{r}')u_{\lambda,\zeta}(\mathbf{r}'). \tag{B21}$$

We then see that U^{intra} corresponds to $g_{00}, \tilde{g}_{00}, g_{zz}$ and U^{inter} to $g_{\perp\perp}$. From this we can immediately deduce that the smallest harmonic of the potential contributing to $g_{\perp\perp}$ is $V(|\mathbf{K}-\mathbf{K}'|)$. For U^{intra} we rewrite

$$|u_\lambda|^2 = \frac{1}{2}(|u_A|^2+|u_B|^2)+\frac{\lambda}{2}(|u_A|^2-|u_B|^2), \tag{B22}$$

giving

$$U^{\text{intra}}_{\lambda\lambda'}(\mathbf{q}) \equiv \frac{1}{4}\sum_{\mathbf{G}} V(|\mathbf{q}+\mathbf{G}|)\Big\{\Big|\int_{\text{uc}} d\mathbf{r} r' e^{i\mathbf{G}\cdot\mathbf{r}}(|u_{A+}(\mathbf{r})|^2+|u_{B+}(\mathbf{r})|^2)\Big|^2 + \lambda\lambda'\Big|\int_{\text{uc}} d\mathbf{r} e^{i\mathbf{G}\cdot\mathbf{r}}(|u_{A+}(\mathbf{r})|^2-|u_{B+}(\mathbf{r})|^2)\Big|^2 + \lambda\int_{\text{uc}} d\mathbf{r}d\mathbf{r}' e^{i\mathbf{G}\cdot(\mathbf{r}-\mathbf{r}')}(|u_{A+}(\mathbf{r})|^2-|u_{B+}(\mathbf{r})|^2)(|u_{A+}(\mathbf{r}')|^2+|u_{B+}(\mathbf{r}')|^2) + \lambda'\int_{\text{uc}} d\mathbf{r}d\mathbf{r}' e^{i\mathbf{G}\cdot(\mathbf{r}-\mathbf{r}')}(|u_{A+}(\mathbf{r})|^2+|u_{B+}(\mathbf{r})|^2)(|u_{A+}(\mathbf{r}')|^2-|u_{B+}(\mathbf{r}')|^2)\Big\}. \tag{B23}$$

The first and second terms can be identified with g_{00} and g_{zz}, respectively, while the third and fourth are $\tilde{g}_{00}$. It is clear that in the presence of sublattice symmetry the third and fourth terms must vanish as they are odd under the exchange of A and B. Using the fact that the Bloch factors are normalized to 1 we see that the lowest-order contribution to g_{00} is

$$g_{00} = V(q) + \text{higher harmonics}, \tag{B24}$$

while the $\mathbf{G}=0$ contributions for the other terms all vanish since

$$\int_{\text{uc}} d\mathbf{r}(|u_{A+}(\mathbf{r})|^2-|u_{B+}(\mathbf{r})|^2) = 1-1=0. \tag{B25}$$

The lowest contributing harmonics are

$$\begin{aligned} g_{00} &\approx V(q), g_{\perp\perp} \\ &\approx \frac{1}{2}V\left(\frac{4\pi}{3a}\right)\sum_i\left(\left|\int_{uc} d\mathbf{r}\cos(\mathbf{b}_i\cdot\mathbf{r})([u_{A+}(\mathbf{r})]^2+[u_{B+}(\mathbf{r})]^2)\right|^2+\left|\int_{uc} d\mathbf{r}\sin(\mathbf{b}_i\cdot\mathbf{r})([u_{A+}(\mathbf{r})]^2+[u_{B+}(\mathbf{r})]^2)\right|^2\right), \\ g_{zz} &\approx \frac{1}{2}V\left(\frac{4\pi}{\sqrt{3}a}\right)\sum_{i=1,2,3}\left(\left[\int_{uc} d\mathbf{r}\cos(\mathbf{b}_i\cdot\mathbf{r})(|u_{A+}(\mathbf{r})|^2-|u_{B+}(\mathbf{r})|^2)\right]^2+\left[\int_{uc} d\mathbf{r}\sin(\mathbf{b}_i\cdot\mathbf{r})(|u_{A+}(\mathbf{r})|^2-|u_{B+}(\mathbf{r})|^2)\right]^2\right), \\ \tilde{g}_{00} &\approx \sum_{i=1,2,3} V\left(\frac{4\pi}{\sqrt{3}a}\right)\int_{\text{uc}} d\mathbf{r}d\mathbf{r}'\cos(\mathbf{b}_i\cdot(\mathbf{r}-\mathbf{r}'))(|u_{A+}(\mathbf{r})|^2|u_{A+}(\mathbf{r}')|^2-|u_{B+}(\mathbf{r})|^2|u_{B+}(\mathbf{r}')|^2), \end{aligned} \tag{B26}$$

where $\mathbf{b}_{1,2}$ are the primitive reciprocal lattice vectors and $\mathbf{b}_3=\mathbf{b}_1+\mathbf{b}_2$. In what follows we therefore set $g_{\perp\perp}, g_{zz}, \tilde{g}_{00}$ to constants and replace g_{00} with the long-range part of the Coulomb interaction. Note that as a consequence of the monotonicity of the Coulomb potential, for the hierarchy of scales $q_{\text{TF}}, k_F \ll |\mathbf{K}-\mathbf{K}'|$ we then have

$$V(q\sim k_F) \gg g_{\perp\perp} > g_{zz} > \tilde{g}_{00}. \tag{B27}$$

APPENDIX C: RELAXATION RATES FOR ARBITRARY ANGULAR HARMONIC

With illustrate here the evaluation of Eq. (21). At low temperatures, the particles are restricted to the Fermi surface and we can write the scattering rates as $W^{\mu}_{\pm}(\phi-\phi',\theta)$, where we have defined ϕ, ϕ' as the angles of $\mathbf{p}_i+\mathbf{p}_{i'}$ and $\mathbf{p}_j+\mathbf{p}_{j'}$, respectively, and where $\theta=\sin^{-1}(q/2k_F)$ is the scattering angle. We also reparametrize the linearized deviations in terms of angular harmonics on the Fermi surface:

$$\delta\bar{\rho}^{\mu}(\mathbf{p}_i,\mathbf{r}) \equiv -\frac{\partial n}{\partial\epsilon}\Big|_{\bar{\epsilon}}\sum_m e^{im\phi_i}\eta^{\mu}_m(\mathbf{r}). \tag{C1}$$

Plugging this form into Eq. (21) allows us to straightforwardly obtain the angular harmonics of the collision integral,

$$I^{\mu}_m[\eta^{\mu}] \equiv \nu_F^{-1}\sum_{\mathbf{p}} e^{-im\phi} I^{\mu}_i[\mathbf{p}] = -\frac{1}{\nu_F T}\int \frac{d^2p_i d^2p_j d^2p_{i'} d^2p_{j'}}{(2\pi)^5}\delta\left(\sum_J{}' \mathbf{p}_J\right)\delta\left(\sum_J{}' \epsilon_J\right) n_i n_j (1-n_{i'})(1-n_{j'}) \times \sum_{\pm,m'} e^{-im\phi_i} W^{\mu}_{\pm}(\phi-\phi',\theta)\left(\eta^{\mu}_{i,m'}e^{im'\phi_i} \pm \eta^{\mu}_{j,m'}e^{im'\phi_j} - \eta^{\mu}_{i',m'}e^{im'\phi_{i'}} \mp \eta^{\mu}_{j',m'}e^{im'\phi_{j'}}\right). \tag{C2}$$

The probabilities $W_{\pm}$ entering the collision integral are defined respectively as the probabilities due to scattering of particles with the same quantum number in the associated channel, which are important only for the even modes and the charge channel,

and the scattering of particles with different quantum number in the associated channel. For example, for the spin mode, W_+ describes scattering of particles with the same spin, while W_- describes scattering of particles with opposite spin.

Explicitly,

$$W_+^d = W_{\uparrow\uparrow;++} + 2W^D_{\uparrow\uparrow;+-} + 2W^D_{\uparrow\downarrow;++} + 2W^D_{\uparrow\downarrow;+-}, \quad W_+^s = W_{\uparrow\uparrow;++} + 2W^D_{\uparrow\uparrow;+-},$$
$$W_+^{vz} = W_{\uparrow\uparrow;++} + 2W^D_{\uparrow\downarrow;++}, \quad W_+^{mz} = W_{\uparrow\uparrow;++} + 2W^D_{\uparrow\downarrow;+-}, \quad W_+^{v\parallel} = W_{\uparrow\uparrow;++} + 2W^{xD}_{\uparrow\downarrow;++}, \quad W_+^{m\parallel} = W_{\uparrow\uparrow;++} + 2W^{xD}_{\uparrow\downarrow;+-}, \tag{C3}$$

and

$$W_-^s = 2(W^D_{\uparrow\downarrow;++} + W^D_{\uparrow\downarrow;+-}), \quad W_-^{vz} = 2(W^D_{\uparrow\uparrow;+-} + W^D_{\uparrow\downarrow;+-}), \quad W_-^{mz} = 2(W^D_{\uparrow\uparrow;+-} + W^D_{\uparrow\downarrow;++}),$$
$$W_-^{v\parallel} = 2(W^{xD}_{\uparrow\uparrow;+-} + W^{xD}_{\uparrow\downarrow;+-}), \quad W_-^{m\parallel} = 2(W^{xD}_{\uparrow\uparrow;+-} + W^{xD}_{\uparrow\downarrow;++}), \tag{C4}$$

where $W^D_{\sigma\sigma';\zeta\zeta'}$ is the scattering probability for two *distinguishable* particles [28,57] with spins σ, σ' and valley indices ζ, ζ', $W_{\uparrow\uparrow;++}$ is the scattering probability for two *indistinguishable* particles in the same spin and valley states, and the superscript x indicates the choice of the τ^x eigenbasis in valley space.

We follow here the methodology of Ref. [38], wherein the integral is evaluated for the + terms (consequently we do not repeat the derivation of the + terms here). First we rewrite the δ functions

$$\delta(\epsilon_i + \epsilon_j - \epsilon_{i'} - \epsilon_{j'}) = \int d\omega \delta(\epsilon_i - \epsilon_{i'} - \omega)\delta(\epsilon_j - \epsilon_{j'} + \omega) \tag{C5}$$

and

$$\delta(\mathbf{p}_i + \mathbf{p}_j - \mathbf{p}_{i'} - \mathbf{p}_{j'}) = \int d^2q \delta(\mathbf{p}_i - \mathbf{p}_{i'} - \mathbf{q})\delta(\mathbf{p}_j - \mathbf{p}_{j'} + \mathbf{q}). \tag{C6}$$

Changing variables to

$$\mathbf{p}_i, \mathbf{p}_{i'} = \mathbf{p} + \frac{\mathbf{l}}{2}, \qquad \mathbf{p}_j, \mathbf{p}_{j'} = \mathbf{p}' - \frac{\mathbf{l}'}{2}, \tag{C7}$$

we can resolve the δ functions to find $\mathbf{l} = \mathbf{l}' = \mathbf{q}$. We rewrite the momentum integrals in polar coordinates:

$$\int d^2p = \int dp p \oint d\phi. \tag{C8}$$

This transforms the collision integral to

$$I^\mu_{m,-}[\eta^\mu] = -\frac{1}{\nu_F T}\frac{1}{(2\pi)^5}\sum_{m'}\eta^\mu_{m'}\int dppdp'p'd\omega \int dqq \oint d\phi d\phi' d\phi_q \delta(\epsilon_i - \epsilon_{i'} - \omega)\delta(\epsilon_j - \epsilon_{j'} + \omega)$$
$$\times n_i n_j (1 - n_{i'})(1 - n_{j'}) e^{-im\phi_i} W^\mu_-(\phi - \phi', \theta)(e^{im'\phi_i} - e^{im'\phi_{i'}} - e^{im'\phi_j} + e^{im'\phi_{j'}}). \tag{C9}$$

The difference of energies appearing in the δ functions can be written as

$$\begin{aligned}\epsilon_i - \epsilon_{i'} &= \epsilon(\mathbf{p} + \mathbf{q}/2) - \epsilon(\mathbf{p} - \mathbf{q}/2) \\ &= \sqrt{v^2p^2 + \frac{v^2q^2}{4} + v^2qp\cos(\phi - \phi_q) + \Delta^2} - \sqrt{v^2p^2 + \frac{v^2q^2}{4} - v^2qp\cos(\phi - \phi_q) + \Delta^2} \\ &= \epsilon\left[\sqrt{1 + \frac{v^2qp}{\epsilon^2}\cos(\phi - \phi_q)} - \sqrt{1 - \frac{v^2qp}{\epsilon^2}\cos(\phi - \phi_q)}\right] \equiv \delta\epsilon,\end{aligned} \tag{C10}$$

where we have defined

$$\epsilon \equiv \sqrt{v^2p^2 + \Delta^2 + \frac{v^2q^2}{4}}. \tag{C11}$$

The δ function may then be written $\delta(\delta\epsilon - \omega)$. Projected to the Fermi surface, the convexity of the square root implies that

$$\delta\epsilon(\phi) = 0 \Rightarrow \cos(\phi - \phi_q) = 0. \tag{C12}$$

This allows us to approximate the δ functions:

$$\delta(\delta\epsilon - \omega) \approx \frac{1}{|\partial\delta\epsilon/\partial\cos(\phi - \phi_q)|}\delta(\cos(\phi - \phi_q)) \approx \sum_{\chi=\pm}\frac{\mu}{v^2qp|\sin(\phi - \phi_q)|}\delta\Big(\phi - \phi_q - \chi\frac{\pi}{2}\Big),$$
$$\delta(\delta\epsilon' - \omega) \approx \frac{1}{|\partial\delta\epsilon'/\partial\cos(\phi' - \phi_q)|}\delta(\cos(\phi' - \phi_q)) \approx \sum_{\chi'=\pm}\frac{\mu}{v^2qp|\sin(\phi' - \phi_q)|}\delta(\phi' - \phi_q - \chi\frac{\pi}{2}). \tag{C13}$$

The Fermi surface value of p can be obtained from

$$p^2 = \frac{\mu^2 - \Delta^2 - v^2\frac{q^2}{4}}{v^2} = p_F^2\left(1 - \frac{q^2}{4p_F^2}\right). \tag{C14}$$

Note that we use μ for chemical potential for compactness of notation here, which is related to Fermi level in the main text by $\mu = E_F + \Delta$. This along with $v_F = \frac{v^2 p_F}{\mu}$ allows us to simplify Eqs. (C13) to

$$\delta(\delta\epsilon - \omega) \approx \sum_{\chi=\pm} \frac{1}{v_F q\sqrt{1-(q/2p_F)^2}}\delta\left(\phi - \phi_q - \chi\frac{\pi}{2}\right), \quad \delta(\delta\epsilon' - \omega) \approx \sum_{\chi'=\pm} \frac{1}{v_F q\sqrt{1-(q/2p_F)^2}}\delta\left(\phi' - \phi_q - \chi'\frac{\pi}{2}\right). \tag{C15}$$

Putting this back in,

$$I^{\mu}_{m,-}[\eta^\mu] = -\frac{1}{v_F v_F^2 T}\frac{1}{(2\pi)^5}\sum_{m'}\eta^{\mu}_{m'}\int dppdpp'd\omega\int\frac{dq}{q(1-(q/2p_F)^2)} \times \sum_{\chi,\chi'}\oint d\phi_q n_i n_j(1-n_{i'})(1-n_{j'})e^{-im\phi_i}W^{\mu}_{-}\left((\chi-\chi')\frac{\pi}{2},\theta\right)(e^{im'\phi_i} - e^{im'\phi_{i'}} - e^{im'\phi_j} + e^{im'\phi_{j'}}). \tag{C16}$$

We now change integration variables to

$$\epsilon = \sqrt{v^2p^2 + \frac{q^2}{4} + \Delta^2}, \qquad \epsilon' = \sqrt{v^2p'^2 + \frac{q^2}{4} + \Delta^2}, \tag{C17}$$

rescale the energy variables by the temperature,

$$\epsilon = \mu + uT, \qquad \epsilon' = \mu + u'T, \qquad \omega = wT, \tag{C18}$$

and change variables for q to

$$\sin\theta = \frac{q}{2k_F} \Rightarrow \frac{dq}{q(1-(q/2p_F)^2)} = \frac{d\theta|\cos\theta|}{\sin\theta\cos^2\theta} = \frac{d\theta}{\sin\theta\cos\theta}. \tag{C19}$$

Then to leading order this renders the collision integral,

$$I^{\mu}_{m,-}[\eta^\mu] = -\sum_{m'}\eta^{\mu}_{m'}\frac{v_F T^2}{v_F^2}\int d\Sigma\int_0^{\pi/2}\frac{d\theta}{\sin\theta\cos\theta} \times \sum_{\chi,\chi'}\oint\frac{d\phi_q}{2\pi}e^{-im\phi_i}W^{\mu}_{-}\left((\chi-\chi')\frac{\pi}{2},\theta\right) \times (e^{im'\phi_i} - e^{im'\phi_{i'}} - e^{im'\phi_j} + e^{im'\phi_{j'}}), \tag{C20}$$

where for compactness we have defined the integration measure

$$d\Sigma = \frac{1}{4\pi^2}dudu'dwn_i n_j(1-n_{i'})(1-n_{j'}). \tag{C21}$$

We now turn to reexpressing the angles ϕ_α in terms of ϕ_q and θ. In general, we have

$$\mathbf{p}_i - \mathbf{p}_{i'} = \mathbf{q} = \mathbf{p}_{j'} - \mathbf{p}_j. \tag{C22}$$

So

$$\sin\left|\frac{\phi_i - \phi_{i'}}{2}\right| = \frac{q}{2k_F} = \sin\theta = \sin\left|\frac{\phi_j - \phi_{j'}}{2}\right| \Rightarrow \left|\frac{\phi_i - \phi_{i'}}{2}\right| = \left|\frac{\phi_j - \phi_{j'}}{2}\right| = \theta, \tag{C23}$$

with the sign determined by the relative direction of $\mathbf{p}$ and $\mathbf{q}$. Since $\phi = \phi_q + \chi\frac{\pi}{2}$,

$$\mathrm{sgn}(\phi_i - \phi_{i'}) = -\chi, \tag{C24}$$

and similarly since $\phi' = \phi_q + \chi'\frac{\pi}{2}$,

$$\mathrm{sgn}(\phi_j - \phi_{j'}) = \chi'. \tag{C25}$$

Thus,

$$\frac{\phi_i - \phi_{i'}}{2} = -\chi\theta, \qquad \frac{\phi_j - \phi_{j'}}{2} = \chi'\theta. \tag{C26}$$

Now for the sums of angles:

$$\tan\phi = \frac{\sin\phi_i + \sin\phi_{i'}}{\cos\phi_i + \cos\phi_{i'}} = \tan\frac{\phi_i + \phi_{i'}}{2} \Rightarrow \phi = \frac{\phi_i + \phi_{i'}}{2}, \tag{C27}$$

$$\tan\phi' = \frac{\sin\phi_j + \sin\phi_{j'}}{\cos\phi_j + \cos\phi_{j'}} = \tan\frac{\phi_j + \phi_{j'}}{2} \Rightarrow \phi' = \frac{\phi_j + \phi_{j'}}{2}. \tag{C28}$$

Combining Eqs. (C26) and (C28) we have

$$\phi_i = \phi - \chi\theta = \phi_q + \chi\left(\frac{\pi}{2} - \theta\right), \quad \phi_{i'} = \phi + \chi\theta = \phi_q + \chi\left(\frac{\pi}{2} + \theta\right), \quad \phi_j = \phi' + \chi'\theta = \phi_q + \chi'\left(\frac{\pi}{2} + \theta\right), \quad \phi_{j'} = \phi' - \chi'\theta = \phi_q + \chi'\left(\frac{\pi}{2} - \theta\right). \tag{C29}$$

We consider the two cases, $\chi = \chi'$ and $\chi = -\chi'$, corresponding to the left- and right-hand diagrams in Fig. 1. When $\chi = \chi'$,

$$\phi = \phi' = \phi_q + \chi\pi/2 \tag{C30}$$

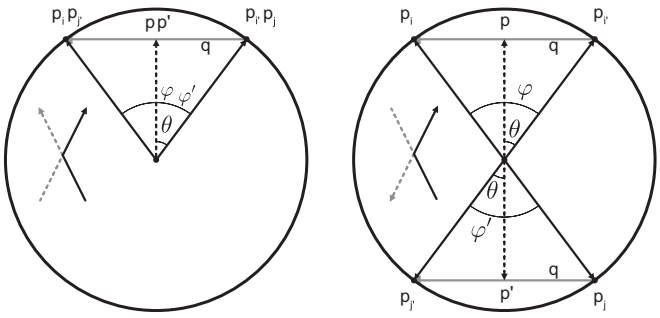

FIG. 1. Position of scattered particles on the Fermi surface and associated angles, for collinear (left) and head-on (right) scattering processes. Note that the momenta $\mathbf{p}$ and $\mathbf{p}'$ do not lie on the Fermi surface.

and we have collinear scattering:

$$\phi_i = \phi_{j'} = \phi_q + \chi\left(\frac{\pi}{2} - \theta\right), \quad \phi_j = \phi_{i'} = \phi_q + \chi\left(\frac{\pi}{2} + \theta\right). \tag{C31}$$

In the other case,

$$\phi = \phi_q + \chi\frac{\pi}{2} = \phi_q - \chi\frac{\pi}{2} + \pi = \phi' + \pi, \tag{C32}$$

which describes head-on scattering:

$$\phi_i = \phi_j + \pi = \phi_q + \chi\left(\frac{\pi}{2} - \theta\right),$$
$$\phi_{i'} = \phi_{j'} + \pi = \phi_q + \chi\left(\frac{\pi}{2} + \theta\right). \tag{C33}$$

The corresponding contributions to the collision integral are

$$\begin{aligned} I^{\mu;For.}_{m,-}[\eta^\mu] &= -2\sum_{m'}\eta^\mu_{m'}\frac{\nu_F T^2}{v_F^2}\int d\Sigma\int_0^{\frac{\pi}{2}}\frac{d\theta}{\sin\theta\cos\theta}W^\mu_-(0,\theta)\sum_\chi\oint\frac{d\phi_q}{2\pi} \\ &\quad\times e^{-im(\phi_q+\chi\pi/2-\chi\theta)}(e^{im'(\phi_q+\chi\pi/2-\chi\theta)} - e^{im'(\phi_q+\chi\pi/2+\chi\theta)}) \\ &= -2\eta^\mu_m\frac{\nu_F T^2}{v_F^2}\int d\Sigma\int_0^{\frac{\pi}{2}}\frac{d\theta}{\sin\theta\cos\theta}W^\mu_-(0,\theta)\sum_\chi(1-e^{2im\chi\theta}) \\ &= -4\eta^\mu_m\frac{\nu_F T^2}{v_F^2}\int d\Sigma\int_0^{\frac{\pi}{2}}\frac{d\theta}{\sin\theta\cos\theta}W^\mu_-(0,\theta)(1-\cos 2m\theta) \end{aligned} \tag{C34}$$

and

$$\begin{aligned} I^{\mu;H.O.}_{m,-}[\eta^\mu] &= -2\sum_{m'}\eta^\mu_m\frac{\nu_F T^2}{v_F^2}\int d\Sigma\int_0^{\frac{\pi}{2}}\frac{d\theta}{\sin\theta\cos\theta}\sum_\chi W^\mu_-(\pi,\theta)e^{-im(\phi_q+\chi\pi/2-\chi\theta)} \\ &\quad\times(e^{im'(\phi_q+\chi\pi/2-\chi\theta)} - e^{im'(\phi_q+\chi\pi/2+\chi\theta)} - e^{im'(\phi_q+\chi\pi/2-\chi\theta+\pi)} + e^{im'(\phi_q+\chi\pi/2+\chi\theta+\pi)}) \\ &= -2\eta^\mu_m\frac{\nu_F T^2}{v_F^2}\int d\Sigma\int_0^{\frac{\pi}{2}}\frac{d\theta}{\sin\theta\cos\theta}W^\mu_-(\pi,\theta)\sum_\chi\frac{1}{2}(1-e^{im\pi})(1-e^{2im\chi\theta}) \\ &= -4\eta^\mu_m\frac{\nu_F T^2}{v_F^2}\int d\Sigma\int_0^{\frac{\pi}{2}}\frac{d\theta}{\sin\theta\cos\theta}W^\mu_-(\pi,\theta)\frac{1}{2}(1-e^{im\pi})(1-\cos 2m\theta). \end{aligned} \tag{C35}$$

Combining the above two expressions, we can identify the contributions to the scattering rate at order T^2:

$$\frac{1}{\tau^\mu_m} = \frac{8\nu_F T^2}{v_F^2}\int d\Sigma\int_0^{\frac{\pi}{2}}\frac{d\theta}{\sin\theta\cos\theta}\left(W^\mu_-(0,\theta) + \frac{(1-e^{im\pi})}{2}W^\mu_-(\pi,\theta)\right)\sin^2 m\theta. \tag{C36}$$

Separating into even and odd m terms,

$$\frac{1}{\tau^\mu_{m,\text{even}}} = \frac{8\nu_F T^2}{v_F^2}\int d\Sigma\int_0^{\frac{\pi}{2}}\frac{d\theta}{\sin\theta\cos\theta}\sin^2 m\theta(W^\mu_-(0,\theta) + W^\mu_+(\pi,\theta)) \sim T^2\log m \tag{C37}$$

and

$$\frac{1}{\tau^\mu_{m,\text{odd}}} = \frac{8\nu_F T^2}{v_F^2}\int d\Sigma\int_0^{\frac{\pi}{2}}\frac{d\theta}{\sin\theta\cos\theta}\sin^2 m\theta(W^\mu_-(0,\theta) + W^\mu_-(\pi,\theta)), \tag{C38}$$

where we have restored the usual contribution [38] from the + channel for the even modes. Note that Eq. (C40) is logarithmically divergent at $\theta \to \frac{\pi}{2}$, corresponding to $q = 2p_f$, if $W(0,\pi/2) + W(\pi,\pi/2)$ is finite. From Fig. 1, one can see then that the divergence is due to backscattering, $\mathbf{p}_i \to -\mathbf{p}_i$ and $\mathbf{p}_j \to -\mathbf{p}_j$.

These can be put into a more conventional form by writing in terms of the scattering angle $\theta_{\text{sc}} = 2\theta$

$$\frac{1}{\tau^\mu_{m,\text{even}}} = \frac{4\nu_F T^2}{v_F^2}\int d\Sigma\int_0^{\pi}\frac{d\theta_{\text{sc}}}{\sin\theta_{\text{sc}}}(1-\cos m\theta_{\text{sc}})\left(W^\mu_{-,\text{Collinear}}(\theta_{\text{sc}}) + W^\mu_{+,\text{Head On}}(\theta_{\text{sc}})\right) \tag{C39}$$

and

$$\frac{1}{\tau^{\mu}_{m,\mathrm{odd}}} = \frac{4\nu_F T^2}{v_F^2}\int d\Sigma \int_0^{\pi} \frac{d\theta_{\mathrm{sc}}}{\sin\theta_{\mathrm{sc}}}(1-\cos m\theta_{\mathrm{sc}}) \times \left(W^{\mu}_{-,\mathrm{Collinear}}(\theta_{\mathrm{sc}}) + W^{\mu}_{-,\mathrm{Head\ On}}(\theta_{\mathrm{sc}})\right), \quad \text{(C40)}$$

where the subscript "sc" on the rates W is just to show that we are now considering them as functions of θ_{sc}.

The structure of the rates, as a sum of head-on and collinear terms, is a general feature of relaxation in two dimensions, as these are the only collision channels allowed by momentum and energy conservation for fermions on a circular Fermi surface (see, e.g., Ref. [58] or the supplement to Ref. [44]). In the charge channel, the collinear term does not contribute to relaxation [38,39,58] due to the indistinguishability of the scattering particles, but in general any collinear collision of particles with different values of a quantum number contributes to the angular relaxation of the associated channel; e.g., the collinear collision of opposite-spin fermions contributes to the relaxation of the spin channel. Similarly, the head-on collision term vanishes at order T^2 for the charge channel [38], but in general contributes for collisions with differing values of quantum number in the channel of interest.

There are two leading contributions to these integrands. For odd terms, there is a logarithmic divergence at $\theta_{\mathrm{sc}} \to \pi$. For all terms there is also, potentially, a logarithmic contribution from forward scattering due to the long-range Coulomb interaction. Thus to leading logarithmic order the transport lifetimes can be approximated:

$$\frac{1}{\tau^{\mu}_{tr}} \equiv \frac{1}{\tau^{\mu}_{1}} \approx \frac{1}{\tau^{\mu}_{1,\mathrm{Backscatter}}} + \frac{1}{\tau^{\mu}_{1,\mathrm{Forward}}}. \quad \text{(C41)}$$

We evaluate these two contributions separately below.

1. Backscattering contribution

To leading logarithmic order we can resolve the backscattering divergence by taking into account the cutoff on the integration region due to kinematic constraints on particle scattering. To do so, we recall that the energy conservation δ functions Eqs. (C5), (C10), and (C11) imposed the constraint

$$\sqrt{1+y}-\sqrt{1-y} = \frac{\omega}{\epsilon},\ \sqrt{1-y'}-\sqrt{1+y'} = \frac{\omega}{\epsilon}, \quad \text{(C42)}$$

where we have defined

$$y = \frac{v^2 pq}{\epsilon^2}\cos(\phi-\phi_q) \quad \text{(C43)}$$

and as before

$$\epsilon^2 = v^2p^2 + \Delta^2 + \frac{v^2q^2}{4}. \quad \text{(C44)}$$

Expanding to lowest order in $w = \omega/T$,

$$\begin{aligned}\sqrt{1+y}-\sqrt{1-y} &= \sum_{k=0}^{\infty}\binom{1/2}{k}(y^k-(-y)^k)\\ &= 2\sum_{k=0}^{\infty}\binom{1/2}{2k+1}y^{2k+1} = \frac{wT}{\mu+uT}\\ &= \frac{w}{1+uT/\mu}T/\mu \approx w\frac{T}{\mu}. \end{aligned} \quad \text{(C45)}$$

Substituting back in Eq. (C43) we have, to order T/μ,

$$\frac{v^2p_F}{\mu^2}q\sqrt{1-\frac{q^2}{4p_F^2}}\cos(\phi-\phi_q) = \frac{\mu^2-\Delta^2}{\mu^2}\sin\theta_{\mathrm{sc}}\cos(\phi-\phi_q) = w\frac{T}{\mu}. \quad \text{(C46)}$$

Since $|\cos| \leqslant 1$ we must then have

$$\sin\theta_{\mathrm{sc}} \geqslant w\frac{T\mu}{\mu^2-\Delta^2}, \quad \text{(C47)}$$

which acts as a constraint on the integration region. From this we define the cutoff angle

$$\sin\theta_c \approx \theta_c \approx w\frac{T\mu}{\mu^2-\Delta^2}. \quad \text{(C48)}$$

Noting that the dominant region for the measure $d\Sigma$ will come from

$$w \approx 1 + O(T/\mu), \quad \text{(C49)}$$

we then approximate this as

$$\theta_c \approx \frac{T\mu}{\mu^2-\Delta^2}. \quad \text{(C50)}$$

The leading-logarithmic backscattering contribution to the transport time may then be obtained with the change of variables $x = \cos(\theta_{\mathrm{sc}}/2)$ in Eq. (C40):

$$\begin{aligned}\frac{1}{\tau^{\mu}_{1,\mathrm{Backscatter}}} &\approx \int d\Sigma \int_{\theta_c/2}^{1}\frac{dx}{x} \times \frac{2\nu_F T^2}{v_F^2}\left(W^{\mu}_{-,\mathrm{Collinear}}(\pi) + W^{\mu}_{-,\mathrm{Head\ On}}(\pi)\right)\\ &= \frac{2\nu_F T^2}{v_F^2}\int d\Sigma \ln\frac{\mu^2-\Delta^2}{T\mu} \times \left(W^{\mu}_{-,\mathrm{Collinear}}(\pi) + W^{\mu}_{-,\mathrm{Head\ On}}(\pi)\right). \end{aligned} \quad \text{(C51)}$$

Using the fact that

$$T \ll \sqrt{\mu^2-\Delta^2} \Rightarrow T \ll \mu \Rightarrow \ln\frac{\sqrt{\mu^2-\Delta^2}}{T} \gg \ln\frac{\sqrt{\mu^2-\Delta^2}}{\mu}, \quad \text{(C52)}$$

we have

$$\frac{1}{\tau^{\mu}_{1,\mathrm{Backscatter}}} \approx \frac{4\nu_F T^2}{v_F^2}\int d\Sigma \ln\frac{\sqrt{\mu^2-\Delta^2}}{T} \times \left(W^{\mu}_{-,\mathrm{Collinear}}(\pi) + W^{\mu}_{-,\mathrm{Head\ On}}(\pi)\right). \quad \text{(C53)}$$

To evaluate the integral over $d\Sigma$ we rewrite it as

$$\int d\Sigma = \frac{1}{(2\pi)^2}\int du_i f_i(1-f_i) \times \int du_j du_{i'} du_{j'}\delta(u_i+u_j-u_{i'}-u_{j'}) \times \frac{1}{f_i(1-f_i)}f_i f_j(1-f_{i'})(1-f_{j'}), \quad \text{(C54)}$$

where

$$f_i = \frac{1}{1+\exp(u_i)}. \tag{C55}$$

Using the Appendix of Ref. [38] this can be simplified to

$$\int d\Sigma = \frac{1}{(2\pi)^2}\int du_i f_i(1-f_i)\frac{u_i^2+\pi^2}{2} = -\frac{1}{(2\pi)^2}\int du_i \frac{\partial f_i}{\partial u}\frac{u_i^2+\pi^2}{2} = \frac{1}{6}, \tag{C56}$$

giving

$$\frac{1}{\tau^{\mu}_{1,\text{Backscatter}}} \approx \frac{2\nu_F T^2}{3v_F^2}\ln\frac{\sqrt{\mu^2-\Delta^2}}{T} \times \left(W^{\mu}_{-,\text{Collinear}}(\pi) + W^{\mu}_{-,\text{Head On}}(\pi)\right). \tag{C57}$$

2. Forward-scattering contribution

In two dimensions, the phase space for collinear collisions is logarithmically divergent [21,24,59,60]. This being the case, the scattering rate for the unscreened Coulomb interaction gives a divergent contribution to the transport scattering rate, despite the usual $1-\cos\theta_{\text{sc}}$ suppression of forward-scattering contributions. Physically this divergence is cut off by the screening wave vector. In the case where $q_{\text{TF}} \gg 2k_F$ the Coulomb interaction is short ranged and one need not consider the forward-scattering contribution, as it is effectively suppressed by the transport form factor. However, in the limit $q_{\text{TF}} \ll 2k_F$ the region of the integral $\sin\theta_{\text{sc}} \sim q_{\text{TF}}/2k_F$ gives

$$W^{\mu}_{-}(\theta\to 0) \propto \frac{1}{(q+q_{\text{TF}})^2} \propto \frac{1}{\left(\frac{q_{\text{TF}}}{2k_F}+\sin\theta\right)^2}, \tag{C58}$$

leading to a logarithmic contribution proportional to $T^2\log q_{\text{TF}}^{-1}$.

One may see that the Coulomb term enters all the distinguishable rates. Its leading logarithmic behavior then provides the forward-scattering contribution

$$\frac{1}{\tau^{\mu}_{1,\text{Forward}}} \approx 2^6\frac{(2\pi e^2)^2}{\kappa^2}\frac{\nu_F T^2}{v_F^2}\int d\Sigma \times \int_{\frac{\theta_c}{2}}^{\frac{\pi}{2}-\frac{\theta_c}{2}} d\theta \frac{\tan\theta}{(q_{\text{TF}}+2k_F\sin\theta)^2}, \tag{C59}$$

where κ is the background dielectric constant and the leading prefactor $2^6 = 8\times 2\times 2\times 2$ comes from the prefactor of the relaxation rate, the factor of 2 for distinguishable particles, the sum over forward and head-on collisions, and finally the two different eigenvalue-changing channels. Defining the effective fine-structure constant $\alpha = (e^2/\kappa v)$, we can rewrite

$$\frac{1}{\tau^{\mu}_{1,\text{Forward}}} \approx 2^6\times 4\pi^2\alpha^2\frac{\nu_F T^2 v^2}{v_F^2}\int d\Sigma \times \int_{\frac{\theta_c}{2}}^{\frac{\pi}{2}-\frac{\theta_c}{2}} d\theta \frac{\tan\theta}{(q_{\text{TF}}+2k_F\sin\theta)^2}. \tag{C60}$$

Letting $x = \sin\theta$,

$$\frac{1}{\tau^{\mu}_{1,\text{Forward}}} \approx 2^6\times \pi^2\alpha^2\frac{\nu_F T^2 v^2}{v_F^2}\int d\Sigma \times \int_{\sin\frac{\theta_c}{2}}^{\cos\frac{\theta_c}{2}} \frac{dx}{1-x^2}x\frac{1}{(x+a)^2}, \tag{C61}$$

where we have defined $a = q_{\text{TF}}/2k_F \ll 1$. Extracting the logarithmic divergence due to the Coulomb potential, we have

$$\frac{1}{\tau^{\mu}_{1,\text{Forward}}} \approx 2^6\times \pi^2\alpha^2\frac{\nu_F T^2 v^2}{k_F^2 v_F^2}\int d\Sigma \times \int_{\frac{\theta_c}{2}}^{1} dx\frac{x}{(x+a)^2}. \tag{C62}$$

In principle, as this term is dominated by small angle scattering, dynamical screening effects may become relevant [44]. However, when $T \ll vq_{\text{TF}}$ the logarithmic divergence is cut off by the Thomas-Fermi wave vector before dynamic screening becomes relevant and we are justified in using the static screening approximation. We henceforth work in this limit and subsequently neglect the cutoff angle θ_c for forward scattering as it does not contribute at leading logarithmic order. Changing variables to $y = x + a$,

$$\frac{1}{\tau^{\mu}_{1,\text{Forward}}} \approx 2^6\times \pi^2\alpha^2\frac{\nu_F T^2 v^2}{k_F^2 v_F^2}\int d\Sigma\int_a^1 dy\frac{y-a}{y^2} = 2^6\times \pi^2\alpha^2\frac{\nu_F T^2 v^2}{k_F^2 v_F^2}\int d\Sigma\ln\frac{\sqrt{\mu^2-\Delta^2}}{vq_{\text{TF}}}, \tag{C63}$$

where we have used

$$\sqrt{\mu^2-\Delta^2} = vk_F. \tag{C64}$$

Performing the integral over $d\Sigma$, we then have

$$\frac{1}{\tau^{\mu}_{1,\text{Forward}}} \approx \frac{2^6\pi^2\alpha^2}{6}\frac{v^4}{v_F^2}\frac{\nu_F T^2}{v^2k_F^2}\ln\frac{\sqrt{\mu^2-\Delta^2}}{vq_{\text{TF}}}. \tag{C65}$$

Making use of

$$v_F = \frac{v^2k_F}{\mu}, \qquad \nu_F = \frac{\mu}{2\pi v^2}, \tag{C66}$$

we have

$$\frac{v^4}{v_F^2}\nu_F = \frac{\mu^3}{2\pi v^2k_F^2} = \frac{\mu}{2\pi}\frac{\mu^2}{\mu^2-\Delta^2} \tag{C67}$$

and arrive at

$$\frac{1}{\tau^{\mu}_{1,\text{Forward}}} \approx \frac{2^4\pi\alpha^2}{3}\mu\frac{\mu^2T^2}{(\mu^2-\Delta^2)^2}\ln\frac{\sqrt{\mu^2-\Delta^2}}{vq_{\text{TF}}}. \tag{C68}$$

APPENDIX D: EVALUATION OF THE BACKSCATTERING PROBABILITIES $W^{\mu}(\pi)$

In this section we approximate the probability for backscattering in each channel, appearing in Eq. (C57) for the nonrelativistic case $\Delta \gtrsim E_F$ and the relativistic case $\Delta \ll E_F$.

As noted in Eqs. (22) and (23), the scattering probabilities W^{μ} entering the collision integral can be expressed in terms of the interaction functions U^{μ}, Eq. (5). Using Eq. (A12), we

may estimate these rates in terms of the long-range part of the Coulomb interaction $V(q)$ and the short-range interaction constants $g_{00}, g_{\perp\perp}, g_{zz}, \tilde{g}_{00}$.

As noted above, the backscattering contribution will contain the collinear $\mathbf{p} = \mathbf{p}'$, $\mathbf{q} = -2\mathbf{p}$ and head-on $\mathbf{p} = -\mathbf{p}'$, $\mathbf{q} = 2\mathbf{p}$ terms, as depicted in Fig. 1. Looking at this figure, it is clear that for $\theta = \pi$, the head-on and collinear terms should be equal.

Combining Eqs. (23), (A12), and (A13) we find the combined collinear and head-on contributions in each channel $W^{\mu}_{\rm BS} = W^{\mu}_{-,\rm Collinear}(\pi) + W^{\mu}_{-,\rm Head\ On}(\pi)$ are

$$
\begin{aligned}
W^{s}_{\rm BS} &= 8\left|g_{zz} + \frac{\Delta}{\mu}\tilde{g}_{00} + V_{2k_F}\frac{\Delta^2}{\mu^2}^2\right|,\\
W^{vz}_{\rm BS} = W^{mz}_{\rm BS} &= 4\left(\left|g_{zz} + \frac{\Delta}{\mu}\tilde{g}_{00} + V_{2k_F}\frac{\Delta^2}{\mu^2} - 2g_{\perp\perp}\left(1+\frac{\Delta^2}{\mu^2}\right)^2\right| + \left|g_{zz} + \frac{\Delta}{\mu}\tilde{g}_{00} + V_{2k_F}\frac{\Delta^2}{\mu^2}^2\right|\right),\\
W^{v\parallel}_{\rm BS} &= 4\left(\left|g_{zz} + \frac{\Delta}{\mu}\tilde{g}_{00} + V_{2k_F}\frac{\Delta^2}{\mu^2} - 2g_{\perp\perp}\left(1+\frac{\Delta^2}{\mu^2}\right)^2\right| + \left|g_{zz} + \frac{\Delta}{\mu}\tilde{g}_{00} + V_{2k_F}\frac{\Delta^2}{\mu^2} - g_{\perp\perp}\left(1+\frac{\Delta^2}{\mu^2}\right)^2\right|\right),\\
W^{m\parallel}_{\rm BS} &= 4\left(\left|g_{zz} + \frac{\Delta}{\mu}\tilde{g}_{00} + V_{2k_F}\frac{\Delta^2}{\mu^2} - 2g_{\perp\perp}\left(1+\frac{\Delta^2}{\mu^2}\right)^2\right| + \left|g_{zz} + \frac{\Delta}{\mu}\tilde{g}_{00} + V_{2k_F}\frac{\Delta^2}{\mu^2} + g_{\perp\perp}\left(1+\frac{\Delta^2}{\mu^2}\right)^2\right|\right).
\end{aligned}
\tag{D1}
$$

1. Nonrelativistic limit

For the nonrelativistic limit $V(2k_F)$ is the dominant energy scale due to Eq. (8), and we can approximate Eq. (D1) as simply

$$
W^{\mu}_{\rm BS} \approx 8|V(2k_F)|^2\frac{\Delta^4}{\mu^4}. \tag{D2}
$$

Plugging this into Eq. (C57) and combining with Eq. (C68) leads to Eq. (26) of the main text.

2. Relativistic limit

In the relativistic limit, the long-range Coulomb contributions are suppressed by the factor Δ^2/μ^2 and the short-range interaction constants become important. From Eqs. (7) and (8) we see that the leading-order contribution to the scattering rates will be due to $g_{\perp\perp}$ for all channels except the spin channel, where it is absent and g_{zz} is the leading term. We may thus approximate Eq. (D1) as

$$
\begin{aligned}
&W^{s}_{\rm BS} = 2\times|g_{zz}|^2,\quad W^{vz}_{\rm BS} = W^{mz}_{\rm BS} = 2\times 8|g_{\perp\perp}|^2,\\
&W^{v\parallel}_{\rm BS} = W^{m\parallel}_{\rm BS} = 2\times 10|g_{\perp\perp}|^2.
\end{aligned}
\tag{D3}
$$

Again, plugging this into Eq. (C57) and combining with Eq. (C68) leads to Eq. (27) of the main text.

[1] A. H. Castro Neto, F. Guinea, N. M. R. Peres, K. S. Novoselov, and A. K. Geim, The electronic properties of graphene, Rev. Mod. Phys. **81**, 109 (2009).

[2] V. N. Kotov, B. Uchoa, V. M. Pereira, F. Guinea, and A. H. Castro Neto, Electron-electron interactions in graphene: Current status and perspectives, Rev. Mod. Phys. **84**, 1067 (2012).

[3] C. C. Grimes and G. Adams, Observation of Two-Dimensional Plasmons and Electron-Ripplon Scattering in a Sheet of Electrons on Liquid Helium, Phys. Rev. Lett. **36**, 145 (1976).

[4] A. L. Fetter, Electrodynamics of a layered electron gas. I. Single layer, Ann. Phys. **81**, 367 (1973).

[5] D. B. Mast, A. J. Dahm, and A. L. Fetter, Observation of Bulk and Edge Magnetoplasmons in a Two-Dimensional Electron Fluid, Phys. Rev. Lett. **54**, 1706 (1985).

[6] E. M. Lifshitz and L. P. Pitaevski, The normal Fermi liquid, in *Statistical Physics*, edited by E. M. Lifshitz and L. P. Pitaevski (Butterworth-Heinemann, Oxford, 1980), pp. 1–27.

[7] L. Levitov and G. Falkovich, Electron viscosity, current vortices and negative nonlocal resistance in graphene, Nat. Phys. **12**, 672 (2016).

[8] D. A. Bandurin, I. Torre, R. Krishna Kumar, M. Ben Shalom, A. Tomadin, A. Principi, G. H. Auton, E. Khestanova, K. S. Novoselov, I. V. Grigorieva, L. A. Ponomarenko, A. K. Geim, and M. Polini, Negative local resistance caused by viscous electron backflow in graphene, Science **351**, 1055 (2016).

[9] J. A. Sulpizio, L. Ella, A. Rozen, J. Birkbeck, D. J. Perello, D. Dutta, M. Ben-Shalom, T. Taniguchi, K. Watanabe, T. Holder, R. Queiroz, A. Principi, A. Stern, T. Scaffidi, A. K. Geim, and S. Ilani, Visualizing Poiseuille flow of hydrodynamic electrons, Nature **576**, 75 (2019).

[10] M. J. H. Ku, T. X. Zhou, Q. Li, Y. J. Shin, J. K. Shi, C. Burch, L. E. Anderson, A. T. Pierce, Y. Xie, A. Hamo, U. Vool, H. Zhang, F. Casola, T. Taniguchi, K. Watanabe, M. M. Fogler, P. Kim, A. Yacoby, and R. L. Walsworth, Imaging viscous flow of the Dirac fluid in graphene, Nature **583**, 537 (2020).

[11] A. Jenkins, S. Baumann, H. Zhou, S. A. Meynell, D. Yang, K. Watanabe, T. Taniguchi, A. Lucas, A. F. Young, and A. C. B. Jayich, Imaging the breakdown of ohmic transport in graphene, arXiv:2002.05065

[12] W. Han, R. K. Kawakami, M. Gmitra, and J. Fabian, Graphene spintronics, Nat. Nanotechnol. **9**, 794 (2014).

[13] J. R. Schaibley, H. Yu, G. Clark, P. Rivera, J. S. Ross, K. L. Seyler, W. Yao, and X. Xu, Valleytronics in 2D materials, Nat. Rev. Mater. **1**, 16055 (2016).

[14] I. Žutić, J. Fabian, and S. Das Sarma, Spintronics: Fundamentals and applications, Rev. Mod. Phys. **76**, 323 (2004).

[15] A. Avsar, H. Ochoa, F. Guinea, B. Özyilmaz, B. J. van Wees, and I. J. Vera-Marun, Colloquium: Spintronics in graphene and other two-dimensional materials, Rev. Mod. Phys. **92**, 021003 (2020).

[16] E. G. Mishchenko, A. V. Shytov, and B. I. Halperin, Spin Current and Polarization in Impure Two-Dimensional Electron Systems with Spin-Orbit Coupling, Phys. Rev. Lett. **93**, 226602 (2004).

[17] K. Flensberg, T. S. Jensen, and N. A. Mortensen, Diffusion equation and spin drag in spin-polarized transport, Phys. Rev. B **64**, 245308 (2001).

[18] C. P. Weber, N. Gedik, J. E. Moore, J. Orenstein, J. Stephens, and D. D. Awschalom, Observation of spin Coulomb drag in a two-dimensional electron gas, Nature **437**, 1330 (2005).

[19] A. J. Leggett and M. J. Rice, Spin Echoes in Liquid He^3 and Mixtures: A Predicted New Effect, Phys. Rev. Lett. **20**, 586 (1968).

[20] K. Miyake and W. J. Mullin, Spin Diffusion in a Two-Dimensional Degenerate Fermi Liquid, Phys. Rev. Lett. **50**, 197 (1983).

[21] M. Müller and H. C. Nguyen, Collision-dominated spin transport in graphene and Fermi liquids, New J. Phys. **13**, 035009 (2011).

[22] P. San-Jose, A. Gutiérrez-Rubio, M. Sturla, and F. Guinea, Spontaneous strains and gap in graphene on boron nitride, Phys. Rev. B **90**, 075428 (2014).

[23] C. W. J. Beenakker, Colloquium: Andreev reflection and Klein tunneling in graphene, Rev. Mod. Phys. **80**, 1337 (2008).

[24] E. H. Hwang and S. Das Sarma, Single-particle relaxation time versus transport scattering time in a two-dimensional graphene layer, Phys. Rev. B **77**, 195412 (2008).

[25] I. L. Aleiner, D. E. Kharzeev, and A. M. Tsvelik, Spontaneous symmetry breaking in graphene subjected to an in-plane magnetic field, Phys. Rev. B **76**, 195415 (2007).

[26] M. Kharitonov, Phase diagram for the $N = 0$ quantum Hall state in monolayer graphene, Phys. Rev. B **85**, 155439 (2012).

[27] Here we use Σ for the sublattice Pauli matrices and reserve σ for the spin Pauli matrices, as the sublattice degree of freedom will be projected out shortly. This differs from the notation commonly used in the literature of denoting the sublattice Pauli matrices σ and spin Pauli matrices s. We retain the use of τ for valley Pauli matrices.

[28] P. Nozieres and D. Pines, *Theory of Quantum Liquids* (Avalon, Cambridge, MA, 1999).

[29] D. Xiao, W. Yao, and Q. Niu, Valley-Contrasting Physics in Graphene: Magnetic Moment and Topological Transport, Phys. Rev. Lett. **99**, 236809 (2007).

[30] J.-Y. Chen and D. T. Son, Berry Fermi liquid theory, Ann. Phys. **377**, 345 (2017).

[31] F. Stern, Polarizability of a Two-Dimensional Electron Gas, Phys. Rev. Lett. **18**, 546 (1967).

[32] E. H. Hwang and S. Das Sarma, Dielectric function, screening, and plasmons in two-dimensional graphene, Phys. Rev. B **75**, 205418 (2007).

[33] A. Lucas and S. Das Sarma, Electronic sound modes and plasmons in hydrodynamic two-dimensional metals, Phys. Rev. B **97**, 115449 (2018).

[34] E. M. Lifšic, L. P. Pitaevskij, L. D. Landau, and E. M. Lifshitz, *Statistical Physics. Part 2. Theory of the Condensed State*, edited by E. M. Lifshitz and L. P. Pitaevski, Course of Theoretical Physics Vol. 9 (Elsevier, Oxford, 2006), p. 387.

[35] A. Klein, D. L. Maslov, L. P. Pitaevskii, and A. V. Chubukov, Collective modes near a Pomeranchuk instability in two dimensions, Phys. Rev. Research **1**, 033134 (2019).

[36] A. Klein, D. L. Maslov, and A. V. Chubukov, Hidden and mirage collective modes in two dimensional Fermi liquids, npj Quantum Mater. **5**, 55 (2020).

[37] E. H. Hwang and S. Das Sarma, Screening-induced temperature-dependent transport in two-dimensional graphene, Phys. Rev. B **79**, 165404 (2009).

[38] P. J. Ledwith, H. Guo, and L. Levitov, The hierarchy of excitation lifetimes in two-dimensional Fermi gases, Ann. Phys. **411**, 167913 (2019).

[39] P. Ledwith, H. Guo, and L. Levitov, Angular superdiffusion and directional memory in two-dimensional electron fluids, arXiv:1708.01915.

[40] Because of the time-reversal symmetry of the system this is equivalent to calculating $\tau_{\rm tr}^{\mu} \equiv \tau_1^{\mu}$.

[41] D. Menashe and B. Laikhtman, Quasiparticle lifetime in a two-dimensional electron system in the limit of low temperature and excitation energy, Phys. Rev. B **54**, 11561 (1996).

[42] We perform calculations in the static screening approximation. Dynamic screening effects are unimportant so long as we remain at low temperatures $vq_{\rm TF} \gg T$ (see Appendix C 2), but see Ref. [43] and the supplement to Ref. [44] for discussion of the effects of dynamic screening.

[43] G. Zala, B. N. Narozhny, and I. L. Aleiner, Interaction corrections at intermediate temperatures: Longitudinal conductivity and kinetic equation, Phys. Rev. B **64**, 214204 (2001); B. N. Narozhny, G. Zala, and I. L. Aleiner, Interaction corrections at intermediate temperatures: Dephasing time, *ibid.* **65**, 180202(R) (2002).

[44] P. S. Alekseev and A. P. Dmitriev, Viscosity of two-dimensional electrons, Phys. Rev. B **102**, 241409(R) (2020).

[45] D. A. Abanin, A. V. Shytov, L. S. Levitov, and B. I. Halperin, Nonlocal charge transport mediated by spin diffusion in the spin Hall effect regime, Phys. Rev. B **79**, 035304 (2009).

[46] M. Yamamoto, Y. Shimazaki, I. V. Borzenets, and S. Tarucha, Valley Hall effect in two-dimensional hexagonal lattices, J. Phys. Soc. Jpn. **84**, 121006 (2015).

[47] R. V. Gorbachev, J. C. W. Song, G. L. Yu, A. V. Kretinin, F. Withers, Y. Cao, A. Mishchenko, I. V. Grigorieva, K. S. Novoselov, L. S. Levitov, and A. K. Geim, Detecting topological currents in graphene superlattices, Science **346**, 448 (2014).

[48] J. Ingla-Aynés, M. H. D. Guimarães, R. J. Meijerink, P. J. Zomer, and B. J. van Wees, 24-μm spin relaxation length in boron nitride encapsulated bilayer graphene, Phys. Rev. B **92**, 201410(R) (2015).

[49] M. Gurram, S. Omar, and B. J. van Wees, Electrical spin injection, transport, and detection in graphene-hexagonal boron

nitride van der Waals heterostructures: Progress and perspectives, 2D Mater. **5**, 032004 (2018).

[50] A. Liu and A. M. Finkel'stein, Valley current in graphene through electron-phonon interaction, Phys. Rev. B **101**, 241401(R) (2020).

[51] M. Lee, J. R. Wallbank, P. Gallagher, K. Watanabe, T. Taniguchi, V. I. Fal'ko, and D. Goldhaber-Gordon, Ballistic miniband conduction in a graphene superlattice, Science **353**, 1526 (2016).

[52] M. M. Glazov and E. L. Ivchenko, Precession spin relaxation mechanism caused by frequent electron-electron collisions, JETP Lett. **75**, 403 (2002).

[53] See Eq. (25) in M. M. Glazov and E. L. Ivchenko, Effect of electron-electron interaction on spin relaxation of charge carriers in semiconductors, J. Exp. Theor. Phys. **99**, 1279 (2004).

[54] See, for example, Z. Wang, D.-K. Ki, J. Y. Khoo, D. Mauro, H. Berger, L. S. Levitov, and A. F. Morpurgo, Origin and Magnitude of "Designer" Spin-Orbit Interaction in Graphene on Semiconducting Transition Metal Dichalcogenides, Phys. Rev. X **6**, 041020 (2016).

[55] G. Tarnopolsky, A. J. Kruchkov, and A. Vishwanath, Origin of Magic Angles in Twisted Bilayer Graphene, Phys. Rev. Lett. **122**, 106405 (2019).

[56] O. Vafek and J. Kang, Renormalization Group Study of Hidden Symmetry in Twisted Bilayer Graphene with Coulomb Interactions, Phys. Rev. Lett. **125**, 257602 (2020).

[57] V. J. Emery, Low-temperature expansion of the transport coefficients and specific heat of Fermi liquids, Phys. Rev. **170**, 205 (1968).

[58] B. Laikhtman, Electron-electron angular relaxation in a two-dimensional electron gas, Phys. Rev. B **45**, 1259 (1992).

[59] S. Das Sarma and F. Stern, Single-particle relaxation time versus scattering time in an impure electron gas, Phys. Rev. B **32**, 8442 (1985).

[60] M. Müller, J. Schmalian, and L. Fritz, Graphene: A Nearly Perfect Fluid, Phys. Rev. Lett. **103**, 025301 (2009).